Final Copy

INFINITE CONDUCTIVITY FRACTURE

IN A

NATURALLY FRACTURED RESERVOIR

A REPORT SUBMITTED TO

THE DEPARTMENT OF PETROLEUM ENGINEERING

OF STANFORD UNIVERSITY

IN PARTIAL FULFILLMENT OF THE REQUIREMENTS

FOR THE DEGREE OF

MASTER OF SCIENCE

by

Olivier Pierre Houzé

June 1983

ACKNOWLEDGEMENT

Financial support for this study was provided by FLOPETROL, Stanford University, and Department of Energy Grant

I would like to thank Doctor Roland Horne and Doctor Henry Ramey for their precious advises.

Olivier Houzé

ABSTRACT

This report describes the behavior of a naturally fractured reservoir when a well is producing at constant rate through an infinite conductivity fracture.

The reservoir model is a double-porosity medium, as it was presented by Warren and Root (1963). The pseudo-steady state interporosity flow assumption is used. The problem is solved as Gringarten (1972) solved for a single-porosity medium, by solving the uniform flux fracture problem and measuring the pressure at an eccentric point of the fracture.

The line source solution is reviewed and the line Green function is introduced. The resolution of the problem also needs the element source solution and the element Green function (produced by an element of fracture). All these functions are obtained in Laplace space and inverted using the Stehfest (1970) numerical algorithm.

The uniform flux fracture is studied, and a simulation of the problem is tried. Finally, the problem is solved directly from the uniform flux problem. Type-curves are presented.

TABLE OF CONTENTS

LIST OF FIGURES

1. INTRODUCTION

Most solutions of transient flow problems concern the behavior of homogeneous formations. This report is the adaptation of one of these solutions to fissured systems. A study of the behavior of a homogeneous reservoir totally penetrated by a thin vertical fracture of infinite conductivity was presented by Gringarten et al. in 1972. Gringarten et al. solved the fracture problem by cutting the whole fracture in 2M elements, and assumed that the flow from the medium to the fracture is uniform in each element. The values of the flows are computed by equating the pressure of all the elements at any given time t. The conclusion of this study was that the pressure in an infinite conductivity fracture is the same as the pressure in a uniform flux fracture computed at the point $(0.732\ X_F, 0.)$. The solution used Green functions and the Line Source solution, which are analytically known for a homogeneous medium.

The problem is different for a fissured formation. The problem produces two different pressures at the same point. Both Line Source and Line Green problems yield a modified Bessel equation in Laplace space. Solving this equation gives the analytical value of the Laplace transform of the solution. For the time being, it has been impossible to invert the result analytically. The consequence is that we require a numerical inversion (Stehfest algorithm).

Integrating the Line Source solution in the space yield the uniform flux function. The value of this function at the point $0.732\ X_F$ is the pressure for an infinite conductivity fracture.

2. A DOUBLE-POROSITY MEDIUM

We consider the double-porosity medium defined by Warren and Root (1963). A double-porosity reservoir, or naturally-fractured reservoir, consists of two distinct porous media of separate porosities and permeabilities: The matrix medium and the fissures. At each point of the reservoir, there are two pressures: the matrix pressure (p_m) and the fissure pressure (p_f).

Before production, the double-porosity reservoir is in equilibrium ($p_m=p_f=p_i$). When a well is producing, the higher permeability of the fissures creates a difference of pressure between the two media (The well is mainly producing the fissure fluid). Then, fluid flows from the matrix to the fissures. If we neglect the permeability of the matrix, all the flow in the well is produced through the fissures.

The flow from the matrix to the fissures is related to the difference of pressures p_m-p_f. There are different ways to define this flow. We will use the pseudo steady-state assumption of Warren and Root (1963).

The material balance for the fissures can be written:

$$[((\rho u_x)_f)_x-((\rho u_x)_f)_{x+\delta x}]\delta y\delta z\delta t + [\,]\delta x\delta z\delta t + [\,]\delta x\delta y\delta t + \rho_f q^* \delta x\delta y\delta z\delta t = \delta(\rho V\Phi)_f \delta x\delta y\delta z$$

Taking $\delta x, \delta y, \delta z, \delta t \to 0$, we obtain the differential equation:

$$-\left[\frac{\partial(\rho u_x)_f}{\partial x} + \frac{\partial(\rho u_y)_f}{\partial y} + \frac{\partial(\rho u_z)_f}{\partial z} \right] + \rho_f q^* = \frac{\partial(\rho V\Phi)_f}{\partial t} \qquad (2\text{-}1)$$

We assume that Darcy's law is valid: $\vec{u}_f = -\frac{k_f}{\mu}\vec{\nabla}p_f$. So:

$$\frac{k_f}{\mu}\left[\frac{\partial}{\partial x}\left(\rho_f \frac{\partial p_f}{\partial x}\right) + \frac{\partial}{\partial y}\left(\rho_f \frac{\partial p_f}{\partial y}\right) + \frac{\partial}{\partial z}\left(\rho_f \frac{\partial p_f}{\partial z}\right) \right] + \rho_f q^* = \frac{\partial(\rho V\Phi)_f}{\partial t} \qquad (2\text{-}2)$$

We assume that the fluid is slightly compressible:

$$\rho_f = \rho_s\, e^{c(p_f-p_s)}$$

Replacing ρ_f in Eq.2–2 and neglecting terms like $c(\frac{\partial p}{\partial x})^2$, we get:

$$\frac{k_f}{\mu} \nabla^2 p_f + q^* = \frac{1}{\rho_f} \frac{\partial}{\partial t}(\rho V\Phi)_f = V_f \Phi (c+c_f) \frac{\partial p_f}{\partial t} \qquad (2\text{–}3)$$

Calling $c_t = c+c_f$, we get the fissure equation:

$$\frac{k_f}{\mu} \nabla^2 p_f = (V\Phi c_t)_f \frac{\partial p_f}{\partial t} - q^* \qquad (2\text{–}4)$$

Applying the **same** procedure to the matrix medium, and neglecting k_m, we obtain the matrix equation:

$$q^* = -(V\Phi c_t)_m \frac{\partial p_m}{\partial t} \qquad (2\text{–}5)$$

We have ***two*** equations and three unknowns. We use the Warren and Root (1963) assumption **of** pseudo–steady flow from the matrix to the fissures:

$$q^* = \alpha \frac{k_m}{\mu} (p_m - p_f) \qquad (2\text{–}6)$$

Eliminating q^* from Eq.2–4 and Eq.2–5, we obtain the definitive pressure equations:

$$\frac{k_f}{\mu} \nabla^2 p_f = (V\Phi c_t)_f \frac{\partial p_f}{\partial t} + (V\Phi c_t)_m \frac{\partial p_m}{\partial t} \qquad (2\text{–}7)$$

$$\alpha \frac{k_m}{\mu} (p_m - p_f) = -(V\Phi c_t)_m \frac{\partial p_m}{\partial t} \qquad (2\text{–}8)$$

THE NOMENCLATURE IS DEFINED IN SECTION 7.

3. THE FRACTURE PROBLEM

We model a thin (zero-thickness for the reservoir) vertical fracture of total length $2X_F$, totally penetrating a horizontal double-porosity reservoir initially at constant pressure (see Fig.3-1). At time zero, a single-phase, slightly-compressible fluid flows from the reservoir into the fracture at a constant total rate q. The flowing pressure is continuous relative to the fissure pressure of the double-porosity medium.

Under these conditions, the flux per unit area in the fracture may not be uniform, and is determined by the limit conditions and the pressure equations for the matrix and the fissures.

We assume that the fracture has an infinite conductivity. Therefore, the producing pressure remains uniform over the fracture.

We divide the fracture in $2M$ segments of length X_F/M, and assume that the flux per unit area is uniform on each element (see Fig.3-2).

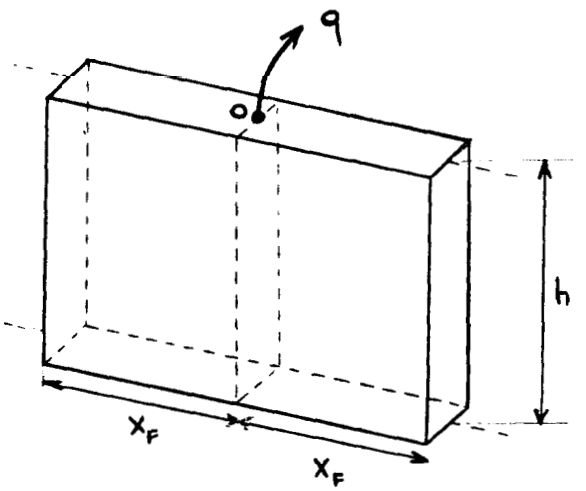

Figure 3-1:
Vertical fracture

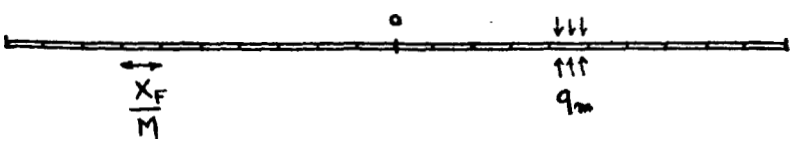

Figure 3-2:
Fracture elements

3.1 Theorical resolution using Green functions

We call LG the line Green function for the double-porosity medium. LG(x,y,t) is the variation of pressure at the point M(x,y) and at time t due to a unit strength source produced at the point 0 at zero time. We call q the total constant rate produced by the well. We call $q_m(\tau)$ the total rate of flow from the medium to the element of fracture number m or (-m) measured at time τ.

The variation of pressure due to the production, measured at the point M(x,y) at time t is:

$$\Delta p(x,y,t) = \int_0^t \sum_{m=1}^{M} \frac{M}{X_F} q_m(\tau) \left[\int_{\frac{(m-1)X_F}{M}}^{\frac{mX_F}{M}} LG(x-x_w,y,t-\tau)dx_w - \int_{-\frac{(m-1)X_F}{M}}^{\frac{mX_F}{M}} LG(x-x_w,y,t-\tau)dx_w \right] d\tau \qquad (3\text{-}1)$$

The values of $q_m(\tau)$ are determined by the equations:

$$\Delta p\left(\frac{2j-1}{2M} X_F, 0., \tau\right) = \Delta p\left(\frac{2j+1}{2M} X_F, 0., \tau\right) \text{ , for } j=1,M-1 \qquad (3\text{-}2)$$

$$2\sum_{m=1}^{M} q_m(\tau) = q \qquad (3\text{-}3)$$

The integrals within the brackets in Eq.3-1 are the Green functions associated with the elements m and (-m).

We call EG the element Green function for a double-porosity medium. EG(x,y,t) is the variation of pressure at the point M(x,y) and at time t due to a uniform source of unit strength produced at time zero by an element of fracture centered in 0. EG is in fact the average of the line Green functions on the element. EG(x,y,t) is given by:

$$EG(x,y,t) = \frac{M}{X_F} \int_{-\frac{X_F}{2M}}^{+\frac{X_F}{2M}} LG(x-x_w,y,t)\, dx_w \qquad (3\text{-}4)$$

Equation 3-1 becomes:

$$\Delta p(x,y,t) = \int_0^t \sum_{m=1}^{M} q_m(\tau) \left[EG\left(x - \frac{2m-1}{2M}X_F, y, t-\tau\right) + EG\left(x + \frac{2m-1}{2M}X_F, y, t-\tau\right) \right] d\tau \qquad (3\text{-}5)$$

3.2 Use of source solutions

The preceeding problem has to be solved by numerical simulation. The rates q_m are assumed constant for a certain interval of time $[t_n, t_{n+1}]$, and the values of q_m are computed from equations 3-2 and 3-3 at time t_{n+1}. An easier way to compute Δp during this period is the use of source solutions.

We call LS the line source solution for a double-porosity medium. LS(x,y,t) is the variation of pressure at the point M(x,y) and at time t due to a continuous rate of one unit produced at the point 0 from time zero to time t. We have:

$$LS(x,y,t) = \int_{\ } LG(x,y,t-\tau)\, d\tau = \int_0^t (x,y,\tau)\, d\tau \qquad (3\text{-}6)$$

Thus :

$$LG(x,y,t) = \frac{\partial LS(x,y,t)}{\partial t} \qquad (3\text{-}7)$$

We will use Eq.3-7 to compute the line Green function from the analytical value of the Laplace transform of the line source solution in Section 4.

We call ES the element source solution for a double-porosity medium. ES(x,y,t) is the variation of pressure at the point M(x,y) and at time t due to a continuous uniform rate of total strength one unit produced from time zero to time t by an element of fracture centered in 0. ES is in fact the average of the line source solutions on the element.

ES is related to LS by:

$$ES(x,y,t) = \frac{M}{X_F} \int_{\frac{-X_F}{2M}}^{\frac{+X_F}{2M}} LS(x-x_w,y,t)\, dx_w \qquad (3\text{-}8)$$

ES is related to EG by:

$$ES(x,y,t) = \int_0^t EG(x,y,t-\tau)\, d\tau = \int_0^t EG(x,y,\tau)\, d\tau \qquad (3\text{-}9)$$

Thus:

$$EG(x,y,t) = \frac{\partial ES(x,y,t)}{\partial t} \qquad (3\text{-}10)$$

If the element m produces at a unit rate from time t_n to time t_{n+1}, the part of the pressure change at the point M(x,y) at time t due to the production of the element during this period will be:

$$\Delta p(x,y,t,n,m) = ES(x-x_m, y, t-t_n) - ES(x-x_m, y, t-t_{n+1}) \qquad (3\text{-}11)$$

Finally, Eq.3-1 becomes:

$$\Delta p(x,y,t_N) = \sum_{n=1}^{N} \sum_{m=1}^{M} q_{n,m} \left[p(x,y,t_N,n,m) + p(x,y,t_N,n,-m) \right] \qquad (3\text{-}12)$$

3.3 Prerequisite to solve the problem

Equation 3-12 and the conditions Eqs.3-2 and 3-3 will be used to produce a simulator describing the behavior of a double-porosity medium in presence of an infinite conductivity fracture. To do this, we need to derive the value of the element source solution ES. The element Green function EG is also needed, as it may be numerically more accurate to compute the solution from small time steps.

In the following sections, we will derive successively LS, LG, EG, ES.

4. LINE SOURCE SOLUTION AND LINE GREEN FUNCTION

The pressure equations 2-7 and 2-8 are written here in two systems of units, Darcy units and English engineering field units:

In Darcy units:

$$\frac{k_f}{\mu}\nabla^2 p_f = (V\Phi c_t)_f \frac{\partial p_f}{\partial t} + (V\Phi c_t)_m \frac{\partial p_m}{\partial t} \tag{4-1a}$$

$$\frac{k_m}{\mu}(p_m - p_f) = -(V\Phi c_t)_m \frac{\partial p_m}{\partial t} \tag{4-2a}$$

In engineering field units:

$$0.000264\frac{k_f}{\mu}\nabla^2 p_f = (V\Phi c_t)_f \frac{\partial p_f}{\partial t} + (V\Phi c_t)_m \frac{\partial p_m}{\partial t} \tag{4-1b}$$

$$0.000264\frac{k_m}{\mu}(p_m - p_f) = -(V\Phi c_t)_m \frac{\partial p_m}{\partial t} \tag{4-2b}$$

We define the following dimensionless variables:

In Darcy units	In engineering field units	
$t_D = \dfrac{k_f t}{[(V\Phi c_t)_f + (V\Phi c_t)_m]\mu X_F^2}$	$t_D = \dfrac{0.000264\, k_f t}{[(V\Phi c_t)_f + (V\Phi c_t)_m]\mu X_F^2}$	(4-3)
$r_D = \dfrac{r}{X_F}$	$r_D = \dfrac{r}{X_F}$	(4-4)
$p_{fD} = \dfrac{2\pi k_f h}{q\mu}(p_i - p_f)$	$p_{fD} = \dfrac{k_f h}{141.2 q\mu B}(p_i - p_f)$	(4-5)
$p_{mD} = \dfrac{2\pi k_f h}{q\mu}(p_i - p_m)$	$p_{mD} = \dfrac{k_f h}{141.2 q\mu B}(p_i - p_m)$	(4-6)

We also define the parameters:

$$\lambda = \alpha \frac{k_m}{k_f} X_F^2 \qquad (4\text{-}7)$$

$$\omega = \frac{(V\Phi c_t)_f}{(V\Phi c_t)_f + (V\Phi c_t)_m} \qquad (4\text{-}8)$$

λ is the interporosity flow parameter. Its value depends on the reference length we choose. ω is the ratio of storativities (ratio of the storativity of the fissures to the storativity of the tital system).

In any system of units, we get the equations:

$$\nabla^2 p_{fD} = \omega \frac{\partial p_{fD}}{\partial t_D} + (1-\omega) \frac{\partial p_{mD}}{\partial t_D} \qquad (4\text{-}9)$$

$$\lambda(p_{mD}-p_{fD}) = -(1-\omega) \frac{\partial p_{mD}}{\partial t_D} \qquad (4\text{-}10)$$

4.1 The line source solution

The line source limit conditions are the same as for a non-zero radius problem, except that the inner boundary condition has to be taken at r_D=0. They can be written:

$$p_{fD}(r_D, t_D=0) = 0 \quad ; \quad p_{mD}(r_D, t_D=0) = 0 \qquad (4\text{-}11)$$

$$\lim_{r_D \to \infty} p_{fD}(r_D, t_D) = 0 \quad , \quad \lim_{r_D \to \infty} p_{mD}(r_D, t_D) = 0 \qquad (4\text{-}12)$$

$$\lim_{r_D \to 0} r_D \frac{\partial p_{fD}}{\partial r_D} = -1 \qquad (4\text{-}13)$$

If we take the Laplace transformation with respect to t_D using Eq.4-11 to compute the Laplace transform of the derivative of p_f and p_m, Eq.4-9 and 4-10 become:

$$\nabla^2 \bar{p}_{fD} = \omega s \bar{p}_{fD} + (1-\omega) s \bar{p}_{mD} \tag{4-14}$$

$$\bar{p}_{mD} = \frac{\lambda}{\lambda + (1-\omega)s} \bar{p}_{fD} \tag{4-15}$$

Substituting Eq.4-15 in 4-14, we get:

$$\nabla^2 \bar{p}_{fD} - sf(s)\bar{p}_{fD} = 0 \tag{4-16}$$

with:

$$f(s) = \frac{\omega(1-\omega)s + \lambda}{(1-\omega)s + \lambda} \tag{4-17}$$

In cylindrical coordinates, Eq.4-16 becomes:

$$\frac{\partial^2 \bar{p}_{fD}}{\partial r_D^2} + \frac{1}{r_D} \frac{\partial \bar{p}_{fD}}{\partial r_D} - sf(s)\bar{p}_{fD} = 0 \tag{4-18}$$

Multiplying by r_D^2, and taking $z = r_D\sqrt{sf(s)}$:

$$z^2 \frac{\partial^2 \bar{p}_{fD}}{\partial z^2} + z \frac{\partial \bar{p}_{fD}}{\partial z} - z^2 \bar{p}_{fD} = 0 \tag{4-19}$$

Equation 4-19 is a modified Bessel equation. The general solution is:

$$\bar{p}_{fD} = A(s)\, I_0(z) + B(s).K_0(s) \tag{4-20}$$

Using the limit condition Eq.4-12 :

$$\lim_{z \to 0} \bar{p}_{fD} = 0 \quad \rightarrow \quad A=0$$

Using the limit condition Eq.4-13 :

$$\lim_{z \to 0} z \frac{\partial \bar{p}_{fD}}{\partial z} = \frac{1}{s} \quad \rightarrow \quad \lim_{z \to 0} zBK_1(z) = \frac{1}{s}$$

When $z \to 0$, $K_1(z) \simeq \frac{1}{z}$, so $B = \frac{1}{s}$.

The Laplace transform of the line source solution for a double-porosity medium is given by:

$$\bar{p}_{fD} = \frac{1}{s} K_o(r_D\sqrt{sf(s)}) \qquad (4\text{-}21)$$

The functions p_f and p_m are obtained from equations 4-15 and 4-21 by the Stehfest(1970) algorithm for numerical inversion.

4.2 The behavior of LS

A Fortran program which computes the line source solution as a function of r_D, t_D, ω and λ is given in appendix. Using double precision was necessary to get good results. The Stehfest algorithm was used with N=16.

A polynomial approximation of K_0 (relative accuracy of 10-7) was first used, but it appeared that this accuracy was insufficant for use of the Stehfest Algorithm, and introduced errors in early time data. Even with an accurate K_0 function, there were still aberations for early time data, but for values of p_f which are negligible in this study. A study of the influence of various parameters is made in the following.

A check was made with the numerical values of LS given by Bruno Deruyck in his master report. The figures were exactly the same, as the function LS was computed the same way.

A LS function result is shown in Fig.4-1. This figure shows the function LS vs $\log(t_D)$ at a given point and for given values of X and ω. At time t_1, the fissured system reaches the semi-log approximation. The curve fits a semi-log straight line till the influence of the matrix system appears at time t_2. From time t_2 to time t_3, we observe a second transition period till the whole system (fissure + matrix) reaches the semi-log approximation (at time t_3).

The familiar line source solution for a single porosity medium is only a function of t_D/r_D^2. We can inspect whether this is true for a double-porosity medium. Figure 4-2 presents the function LS vs $\log(t_D/r_D^2)$ for various values of $\lambda.r_D^2$ (numerical values given in appendix B show that LS is only function of three parameters: t_D/r_D^2, ω,

and λr_D^2). We see that LS is not a function of t_D/r_D^2 alone. The difference arises from the time of the transition period, which is not proportional to r_D^2.

In Fig.4-3, LS is presented vs $\log(t_D)$ for different values of r_D. This figure shows that the time of the transition is almost the same for the different values of r_D. An explanation can be found in the partial differential equations we are using. The pseudo-steady flow assumption (Eq.2-6) yields Eq.2-8 which is not a diffusion equation (no Laplacian term). Therefore, there is no diffusion of the transition.

The influence of λ is shown in Fig.4-2 (we can take r_D constant). It appears that λ determines the time when transition between fissure and matrix control occurs. The Larger λ is, the larger the permeability between the matrix and the fissures is, and the quicker the matrix can react and control the flow. Therefore, the transition occurs earlier for large values of λ. Experimentally, the time of transition is proportional to $1/\lambda$. λ has no influence on the flow curves.

The influence of the storativity ratio ω is shown in Fig.4-4. It appears that ω, which is related to the storativity of the fissures in the medium, determines the duration of the transition between the two semi-log approximations. As ω approaches unity, the medium approaches a single-porosity medium. For $\omega=1$, Eq.4-10 becomes ($p_{mD}=p_{fD}$) and Eq.4-9 becomes the usual diffusivity equation. Thus, the curve ($\omega=1$) is the usual line source solution. For $\omega=0$, we have the limiting case of a zero-storativity fissure system. For a given value of λ, this curve is the envelope of all the transitions.

Fig.4-5 shows flow curves and transition curves for the line source solution. The flow curves are the line source solution for different values of ω and $\lambda=0$ (transition occurs for an infinite time). The transition curves are the line source solution for different values of λ and $\omega=0$. The flow curve for a given value of ω is the homogeneous line source solution with a different scale of time:

$$\text{FLOW}\ (r_D, t_D, \omega) = \text{LS}_{hom}(r_D, t_D/\omega) \qquad (4\text{-}22)$$

Figure 4-1: A typical line source solution

$$t_D = \frac{k_f t}{[(V\Phi c_t)_f + (V\Phi c_t)_m]\mu X_F^2}$$

$$LS = \frac{2\pi k_f h}{q\mu}(p_i - p_f)$$

$$r_D = \frac{r}{X_F} = 1.$$

$$X = 10^{-3}$$

$$\omega = 10^{-2}$$

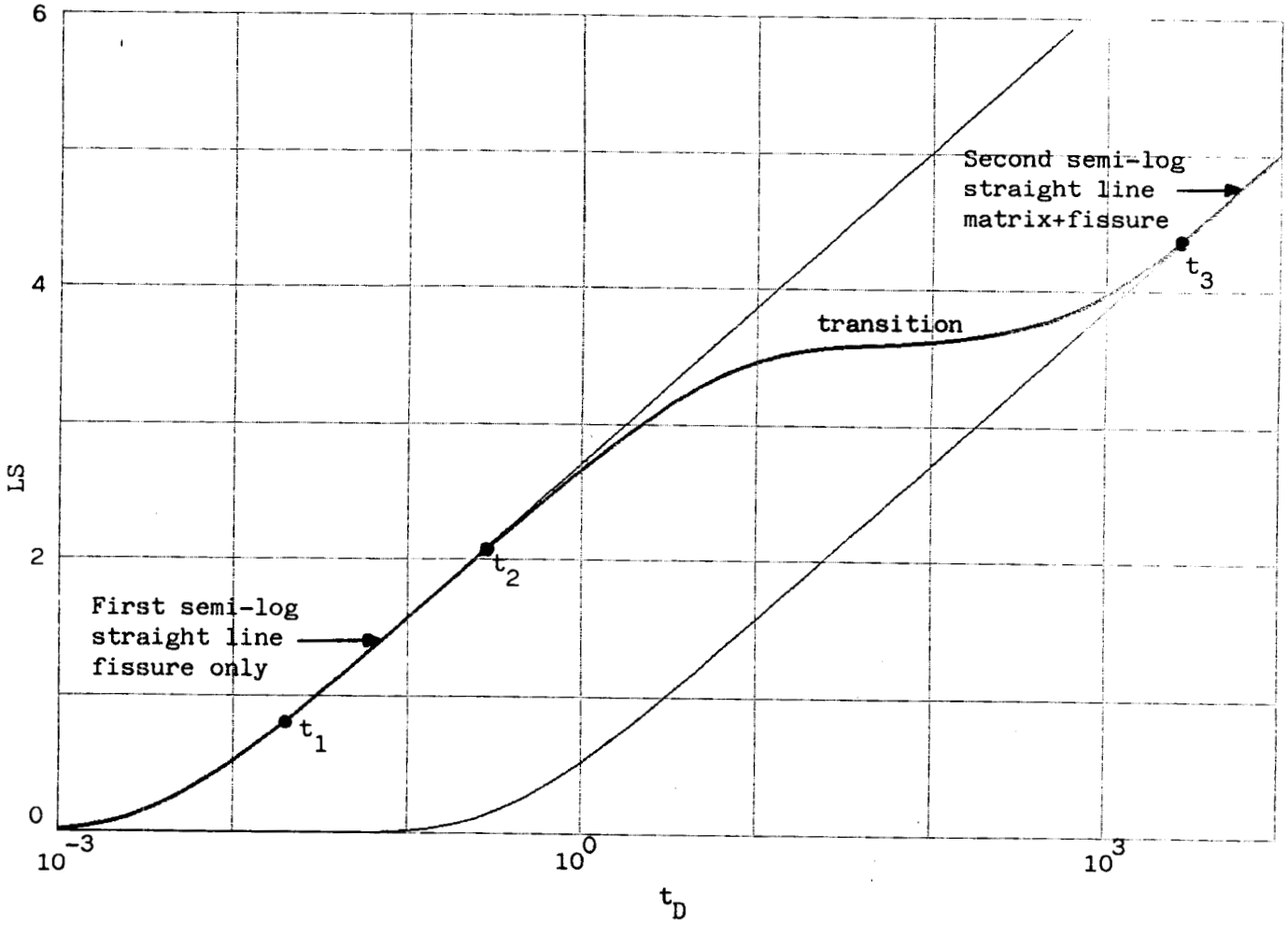

Figure 4-2 : The function LS vs $\log(t_D/r_D^2)$ for various values of $\lambda.r_D^2$

$$t_D/r_D^2 = \frac{k_f t}{[(V\Phi c_t)_f+(V\Phi c_t)_m]\mu r^2}$$

$$LS = \frac{2\pi k_f h}{q\mu}(p_i-p_f)$$

$$\omega = 10^{-2}$$

$$\lambda.r_D^2 = 10^1 \ , \ 10^{-1} \ , \ 10^{-3} \ , \ 10^{-5}$$

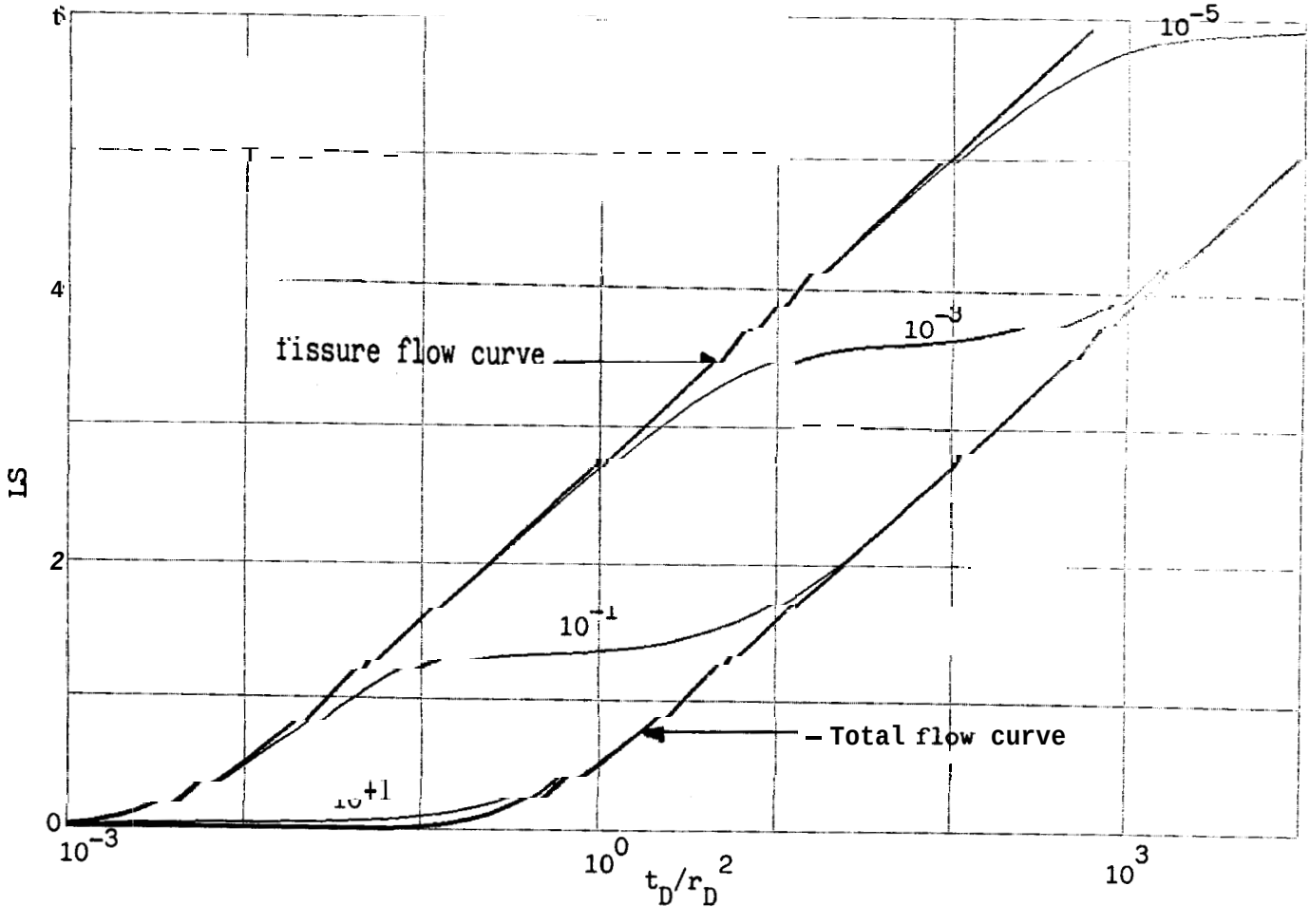

Figure 4-3 : The function LS vs $\log(t_D)$ for various values of r_D

$$t_D = \frac{k_f t}{\{(V\Phi c_t)_f + (V\Phi c_t)_m\}\mu X_F^2}$$

$$LS = \frac{2\pi k_f h}{q\mu}(p_i - p_f)$$

$\omega = 10^{-2}$

$\chi = 10^{-3}$

$rD = 10^{-1}, 10^{0}, 10^{1}, 10^{2}$

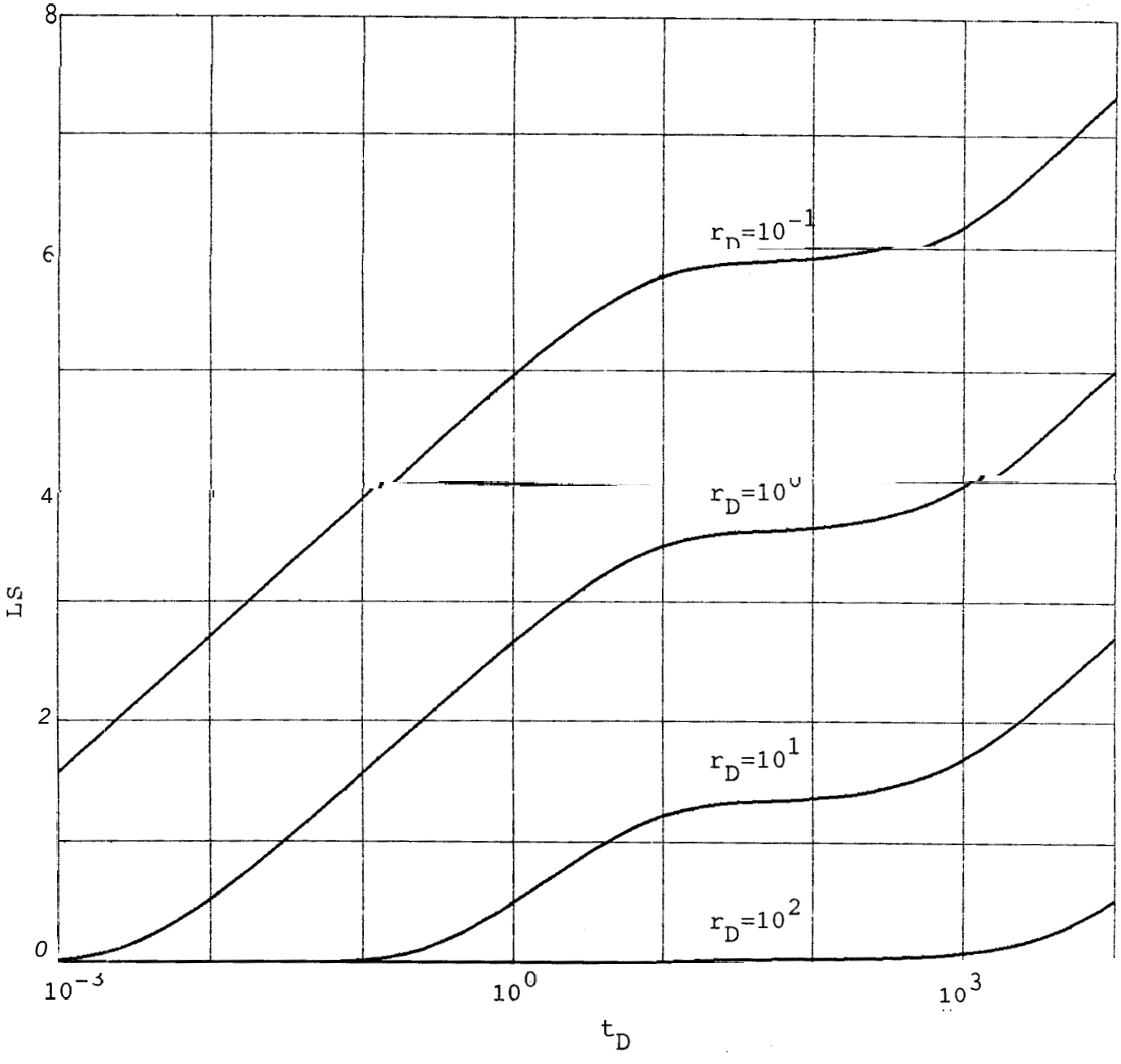

Figure 4-4 : The function LS vs $\log(t_D/r_D^2)$ for various values of ω

$$t_D/r_D^2 = \frac{k_f t}{[(V\Phi c_t)_f+(V\Phi c_t)_m]\mu r^2}$$

$$LS = \frac{2\pi k_f h}{q\mu}(p_i-p_f)$$

$$\lambda . r_D^2 = 10^{-3}$$

$$\omega = 0 \ , \ 10^{-3} \ , \ 10^{-2} \ , \ 10^{-1} \ , \ 1$$

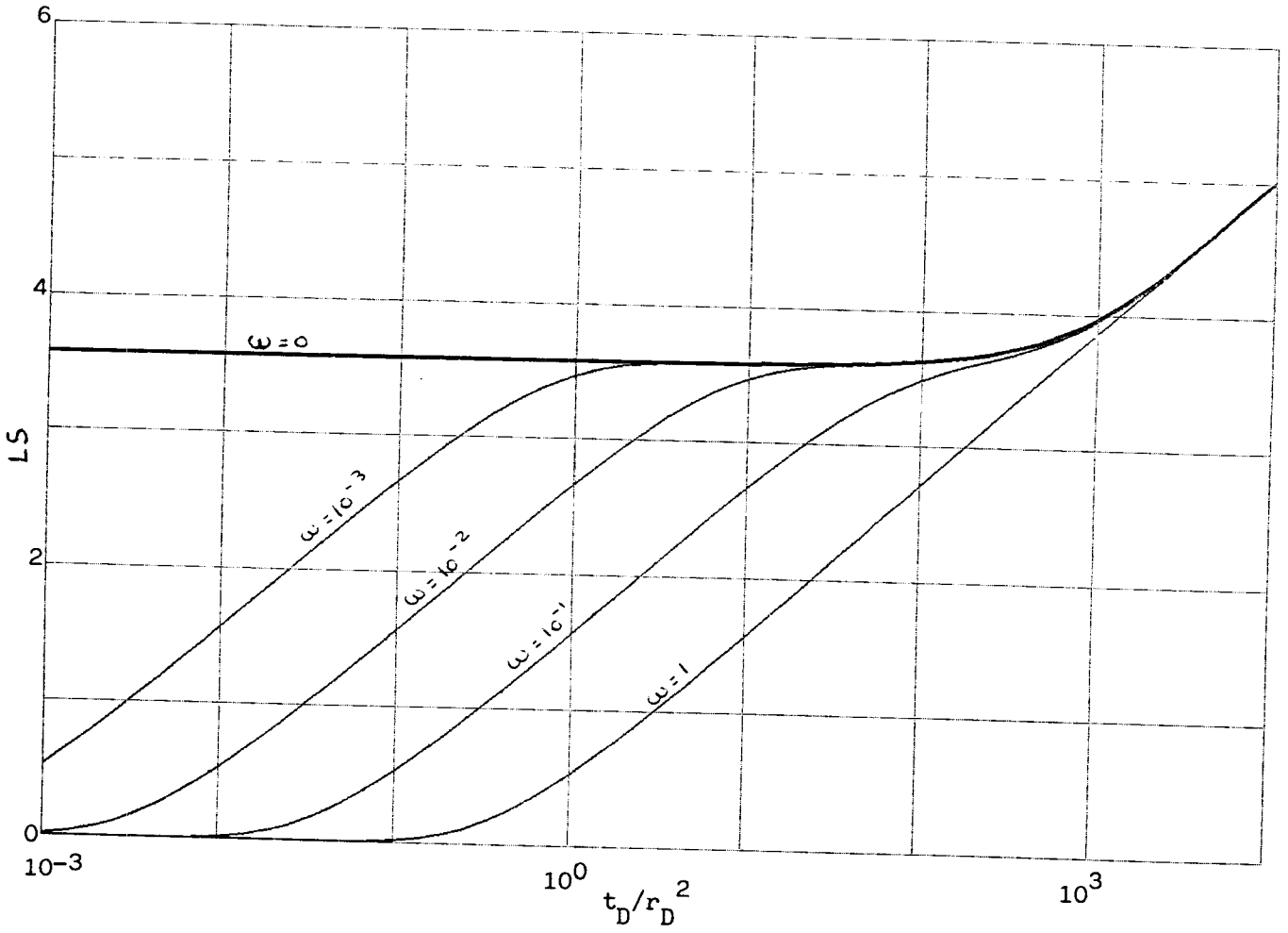

Figure 4-5 : The function **LS** : Flow curves **and** transition enveloppes.

$$t_D/r_D^2 = \frac{k_f t}{\{(V\Phi c_t)_f + (V\Phi c_t)_m\}\mu r^2}$$

$$LS = \frac{2\pi k_f h}{q\mu}(p_i - p_f)$$

Thick curve: $\lambda.r_D^2 = 10^{-3}$ and $\omega = 10^{-2}$

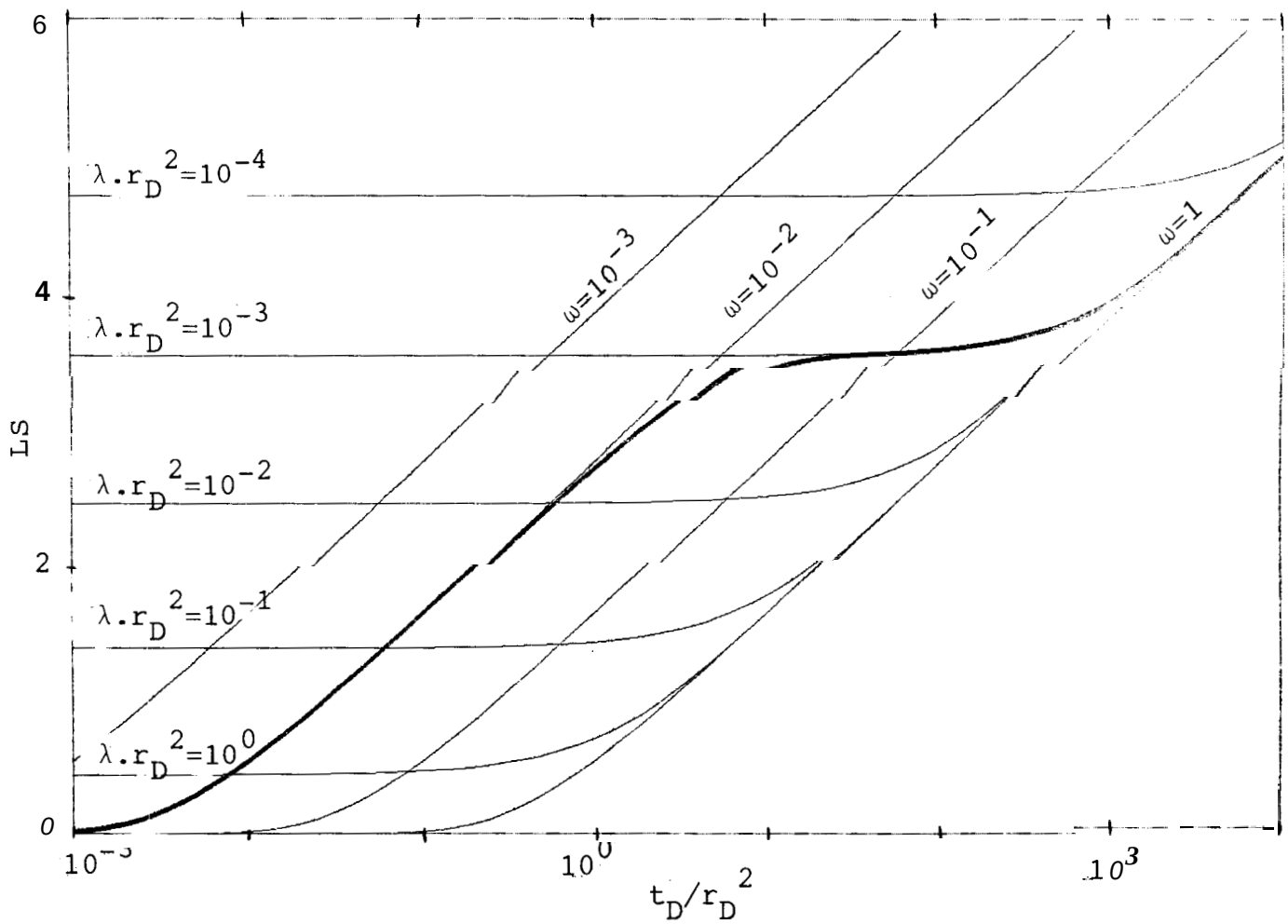

4.3 The line Green function

If we have a constant rate q from $\tau=0$ to $\tau=t$, the value of the fissure pressure p_f at time t is given by the equation:

$$p_i - p_f(r,t) = \frac{q\mu B}{2\pi k_f h} LS(r_D,t_D) \quad \text{in Darcy units} \tag{4-23a}$$

$$p_i - p_f(r,t) = \frac{141.2q\mu B}{k_f h} LS(r_D,t_D) \quad \text{in field units} \tag{4-23b}$$

Supposing we have produced $q(\tau)$ from time τ to time $\tau+d\tau$, the effect of this production at time t will be, using the principle of superposition (Darcy units):

$$\Delta p_f(r,t) = \frac{q\mu B}{2\pi k_f h} \left[LS(r_D,t_D-\tau_D) - LS(r_D,t_D-\tau_D-d\tau_D) \right]$$

Thus:

$$\Delta p_f(r,t) = \frac{q\mu B}{2\pi k_f h} \frac{\partial LS(r_D,t_D-\tau_D)}{\partial(t_D-\tau_D)} d\tau_D \tag{4-24}$$

$LG(r_D,t_D)$ is the dimensionless Green function for a double-porosity medium. It is the dimensionless pressure drop at the point M ($OM_D=r_D$) at time t_D due to a dimensionless source of unit strength produced at the point O at time $t_D=0$.

If we are given the function $q(\tau_D)$ from $\tau_D=0$ to $\tau_D=t_D$, the pressure drop will be:

$$\Delta p_f(r,t) = \frac{\mu B}{2\pi k_f h} \int_0^{t_D} q(\tau_D)\, LG(r_D,t_D-\tau_D)\, d\tau_D \tag{4-25}$$

LG is the derivative of LS with respect to t_D:

$$LG(r_D,t_D) = \frac{\partial LS(r_D,t_D)}{\partial t_D} \tag{4-26}$$

Taking the Laplace transform of Eq.4-26:

$$\overline{LG}(r_D,s) = s.\overline{LS}(r_D,s) \tag{4-27}$$

The value of $\overline{LS}$ is given by Eq.4-21. Thus:

$$\overline{LG}(r_D,s) = K_0(r_D\sqrt{sf(s)}) \qquad (4\text{-}28)$$

LG may be computed by the Stehfest inversion algorithm.

4.4 The behavior of LG

A Fortran program which computes the line Green function as a function of r_D, t_D, ω and λ is given in appendix A. A typical line Green function is shown in Fig.4-6, and compared to the line Green function for a homogeneous reservoir (ω=1). At time t_1, the fissured system reaches a linear log-log approximation. The curve diverges from this log-log straight line only during the transition from time t_2 to time t_3. The importance of Fig.4-6 is that the curve w=l assymptotically fits the double-porosity curve. The analytical form of the single-porosity Green function is given by[7].

$$\text{Green function } (r_D,t_D) = \frac{1}{2t_D}\, e^{-\left[\frac{r_D^2}{4t_D}\right]} \qquad (4\text{-}29)$$

Thus, the log-log straight line is the line ($y = \frac{1}{2t_D}$). This fact permits calculation of LG for very long time, without risk of numerical overflow. It appears even more interesting to study $P_D' = t_D.LG$ than to study EG itself. If we consider LG as the derivative of LS, (4-26) yields:

$$P_D' = t_D \frac{\partial LS(r_D,t_D)}{\partial t_D} = t \frac{\partial LS(r_D,t_D)}{\text{at}} \qquad (4\text{-}30)$$

Thus, using (4-23a), we get the equation:

$$t \frac{\partial p_f}{\partial t} = - \frac{q\mu B}{2\pi k_f h} P_D' \qquad (4\text{-}31)$$

Figure 4-7 shows $\log(P_D')$ vs $\log(t_D/r_D^2)$ for the same values of r_D, ω and λ as in Fig.4-6. The linear log-log approximations are now characterized by a zero slope and $P_D' = ½$

Figure 4-8 shows $\log(P_D')$ vs $\log(t_D/r_D^2)$ for different values of $X.r_D^2$. Figure 4-9 shows the same function for different values of ω. The influence of these parameters is qualitatively the same on LG as on LS.

Figure 4-6 : A typical line Green function

$$t_D/r_D^2 = \frac{k_f t}{\{(V\Phi c_t)_f + (V\Phi c_t)_m\}\mu r^2}$$

$$LG_D = -\frac{2\pi h X_f^2}{\{(V\Phi c_t)_f + (V\Phi c_t)_m\}} \frac{\partial p_f}{}$$

$\omega = 10^{-1}$

$\lambda . r_D^2 = 10^{-3}$

Thin curve: Line Green function for a homogeneous formation (ω=1)

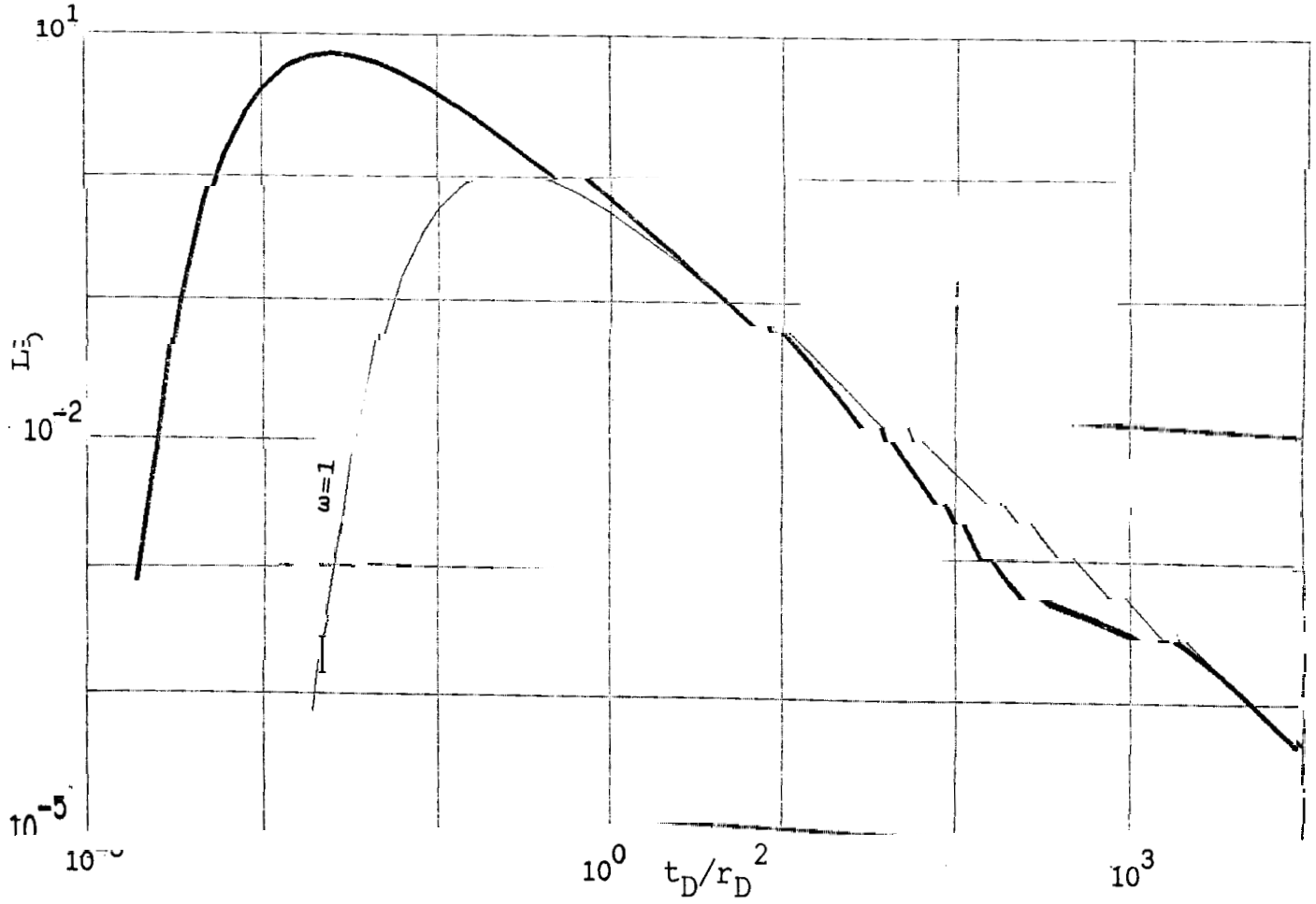

Figure 4-7 : $\log(P_D')$ vs $\log(t_D/r_D^2)$

$$P_D' = t_D \cdot LG = t_D \cdot \frac{\partial LS}{\partial t_D} = - \frac{2\pi k_f h}{q\mu B} \cdot t \frac{\partial p_f}{\partial t}$$

$$t_D/r_D^2 = \frac{k_f t}{[(V\Phi c_t)_f + (V\Phi c_t)_m]\mu r^2}$$

$$\lambda . r_D^2 = 10^{-3}$$

$$\omega = 10^{-1}$$

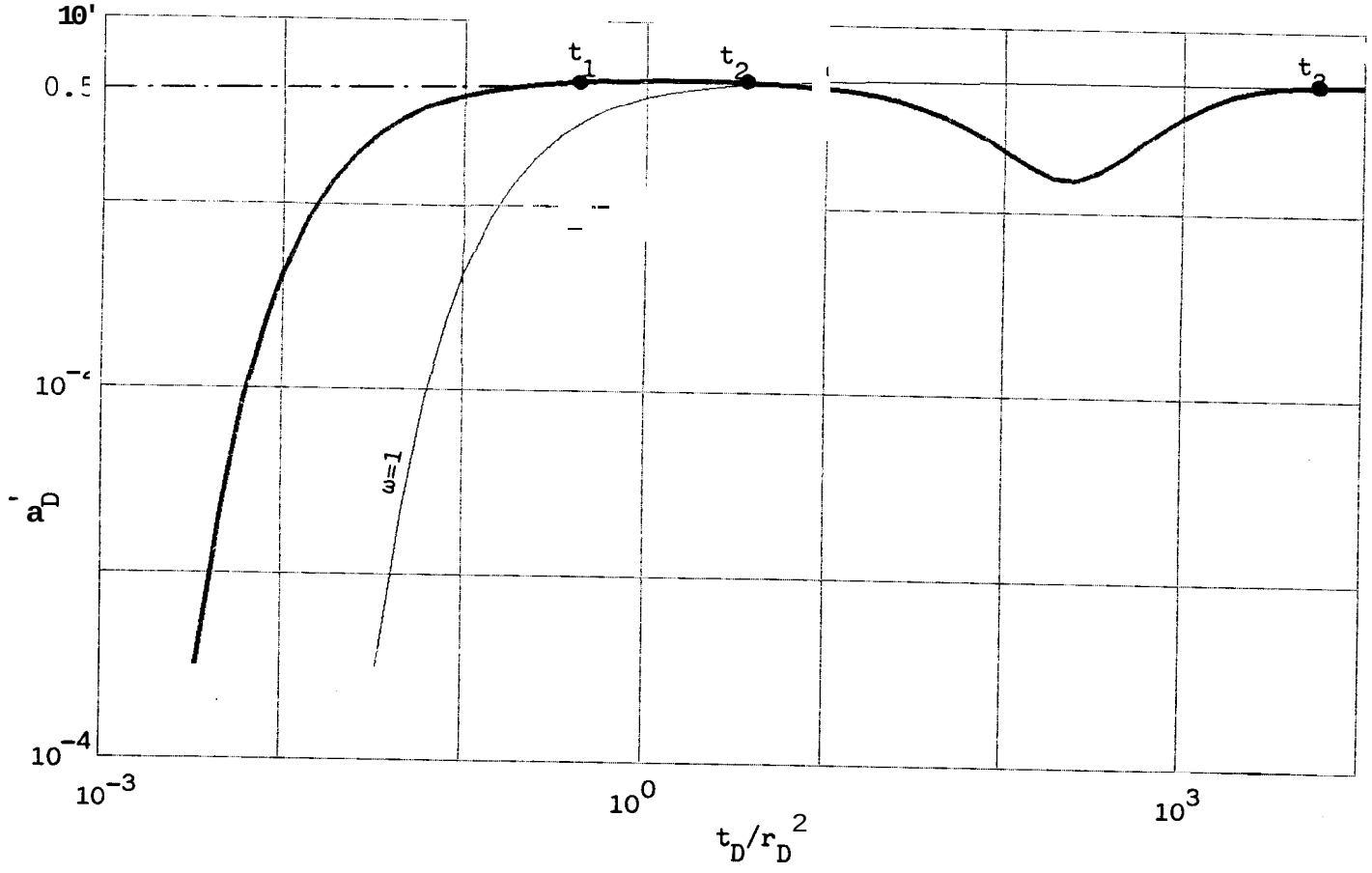

Fiqure 4-8 : Line Green function for different values of $\lambda.r_D^2$

$$P_D' = t_D.LG = t_D.\frac{\partial LS}{\partial t_D} = -\frac{2\pi k_f h}{q\mu B}.\ t\ \frac{\partial p_f}{\partial t}$$

$$t_D/r_D^2 = \frac{k_f t}{((V\Phi c_t)_f+(V\Phi c_t)_m)\mu r^2}$$

$$\omega = 10^{-1}$$

$$\lambda.r_D^2 = 10^1, 10^{-1}, 10^{-3}, 10^{-5}$$

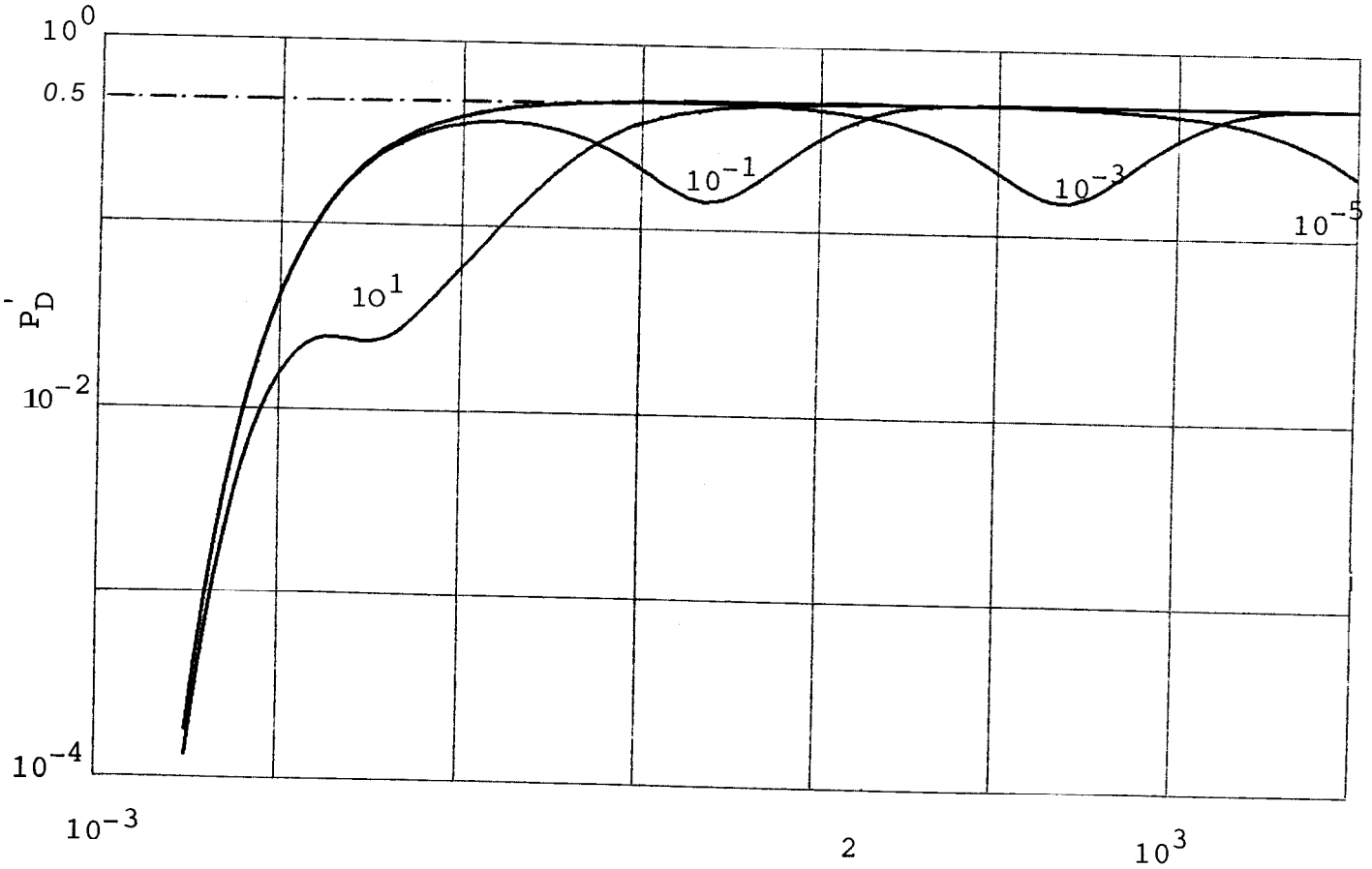

Figure 4-9 : Line Green function for different values of ω

$$P_D' = t_D.LG = t_D.\frac{\partial LS}{\partial t_D} = \frac{2\pi k_f h}{q\mu B}.\ t\ \frac{\partial p_f}{\partial t}$$

$$t_D/r_D^2 = \frac{k_f t}{((V\Phi c_t)_f+(V\Phi c_t)_m)\mu r^2}$$

$$\lambda.r_D^2 = 10^{-3}$$

$$\omega = 10^0, 10^{-1}, 10^{-2}, 10^{-3}$$

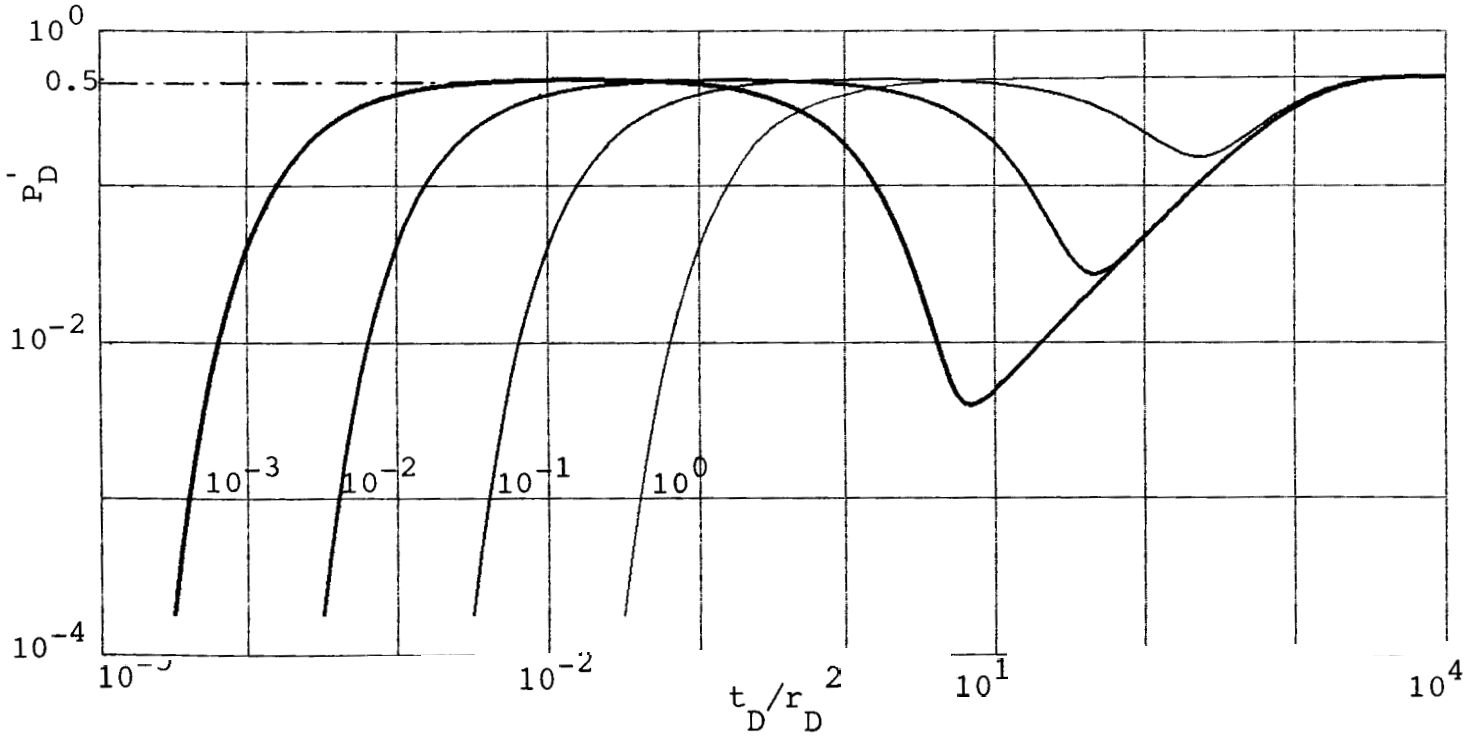

5. ELEMENT GREEN FUNCTION AND ELEMENT SOURCE SOLUTION

5.1 The element Green function

We define EG as the dimensionless element Green function: $EG(x_D,y_D,t_D)$ is the dimensionless pressure drop at the point $M(x_D,y_D)$ at time t_D due to a uniform source of total dimensionless strength 1 produced by an element of fracture centered in 0. The length of this element of fracture is $2X_F/NE$, where NE is the number of elements in the fracture.

EG is the average of the line Green functions on the element. It is given by:

$$EG(x_D,y_D,t_D) = \frac{NE}{2}\cdot\int_{\frac{-1}{NE}}^{\frac{1}{NE}} LG(x_D-u,y_D,t_D)\,du \qquad (5\text{-}1)$$

The analytical value of LG is not known; only its Laplace transform is known, given by Eq.4-28. One way to compute EG is to use the Laplace transform of Eq.5-1. We obtain:

$$\overline{EG}(x_D,y_D,s) = \frac{NE}{2}\cdot\int_{\frac{-1}{NE}}^{\frac{1}{NE}} K_0\left[\sqrt{(x_D-u)^2+y_D^2}\cdot\sqrt{sf(s)}\right]du \qquad (5\text{-}2)$$

If we knew an analytical form of the primitive of K_0, we could perform the integration in Eq.5-2 and use Stehfest algorithm to compute EG. No such form was found in the period of the study.

The way EG was computed was expensive in computer time. We divide the element in NX segments of equal length $2/(NE.NX)$ and assume that the effect of the distribution of flow along each segment is close to the effect of a source of the same strength produced at the center of each segment.

If we call x_i the position of the center of the segment i (i=1,NX), we get:

$$EG(x_D,y_D,t_D) = \frac{1}{NX}\cdot\sum_{i=1}^{NX} LG(x_D-x_i,y_D,t_D) \qquad (5\text{-}3)$$

So, computing one value of EG requires the use of the Stehfest numerical algorithm NX times.

If we want to know the real value of the pressure drop, we use:

$$p_i - p_f(x,y,t) = \frac{qB}{2\pi h[(V\Phi c_t)_f+(V\Phi c_t)_m]X_F^2}\cdot EG(x_D,y_D,t_D) \qquad (5\text{-}4)$$

5.2 The behavior of EG

A typical element Green function is shown in Fig.5-1. $P_D' = t_D.EC$ is plotted versus t_D, and shows the behavior of EG with time at the center of an element for given values of ω and A, and different values of NX. NE is taken equal to one (the element has the length of the fracture). Therefore, this function applies to the behavior of a uniform-flux fracture. The only noticeable influence of NX occurs at early times. The limiting form as $NX\to\infty$ of the early time behavior is a half-slope log-log straight line. At early times, we have:

$$EG = \frac{A}{\sqrt{t_D}} \qquad (5\text{-}5)$$

thus: $$P_D' = A.\sqrt{t_D} \qquad (5\text{-}6)$$

Computing EG for a large value of NX is very expensive in computer time. If we need to compute EG for a large simulation program, we will have to truncate the function. We can use a large value of NX for early time, and a small value of NX for late time.

The influence of A is shown in Fig.5-2. The interporosity flow parameter determines the time of the transition. For large values of A, the transition may occur during the half-slope period (fracture linear flow). The time of the transition is roughly proportional to $1/\lambda$.

The influence of ω is shown in Fig.5-3. The storativity ratio ω has an influence on both early time behavior and transition. For early time, the linear flow curves follow the equation:

$$P'_D = A(\omega).\sqrt{t_D} \qquad \text{or} \qquad EG = \frac{A(\omega)}{\sqrt{t_D}} \tag{5-7}$$

The curve ω=1 is the element Green function for a homogeneous medium. The dimensionless pressure drop for a uniform flux fracture for early time was given by Gringarten et al(1972) :

$$p_D(t_D) = \sqrt{\pi t_D} \tag{5-8}$$

We will see in section 5-3 that $EG=\frac{\partial ES}{\partial t_D}$. p_D being the element source solution for NE=1, we have:

$$EG_{\omega=1}(t_D) = \frac{\sqrt{\pi}}{2\sqrt{t_D}} \quad \text{at early time} \tag{5-9}$$

Thus :

$$A(1) = \frac{\sqrt{\pi}}{2} \tag{5-10}$$

From numerical values, we see that dividing ω by ten translates the early time straight line of one time log cycle on the left. This can be explained by considering that all these curves would be the same if we took the fissure porosity as reference (This will be done in section 6). Therefore, dividing ω by ten corresponds to dividing the fissure porosity by ten, and we have to replace t_D by $10.t_D$.

$$EG_{\omega}(t_D) = \frac{\sqrt{\pi}}{2\sqrt{t_D/\omega}} \tag{5-11}$$

Thus :

$$A(\omega) = \frac{\sqrt{\pi\omega}}{2} \tag{5-12}$$

Figure 5–1 : Element Green function for different values of NX

NE = 1 (uniform flux)

NX = 4,10,30,100

$\omega = 10^{-1}$

$\chi = 10^{-2}$

$P'_D = t_D.EG$

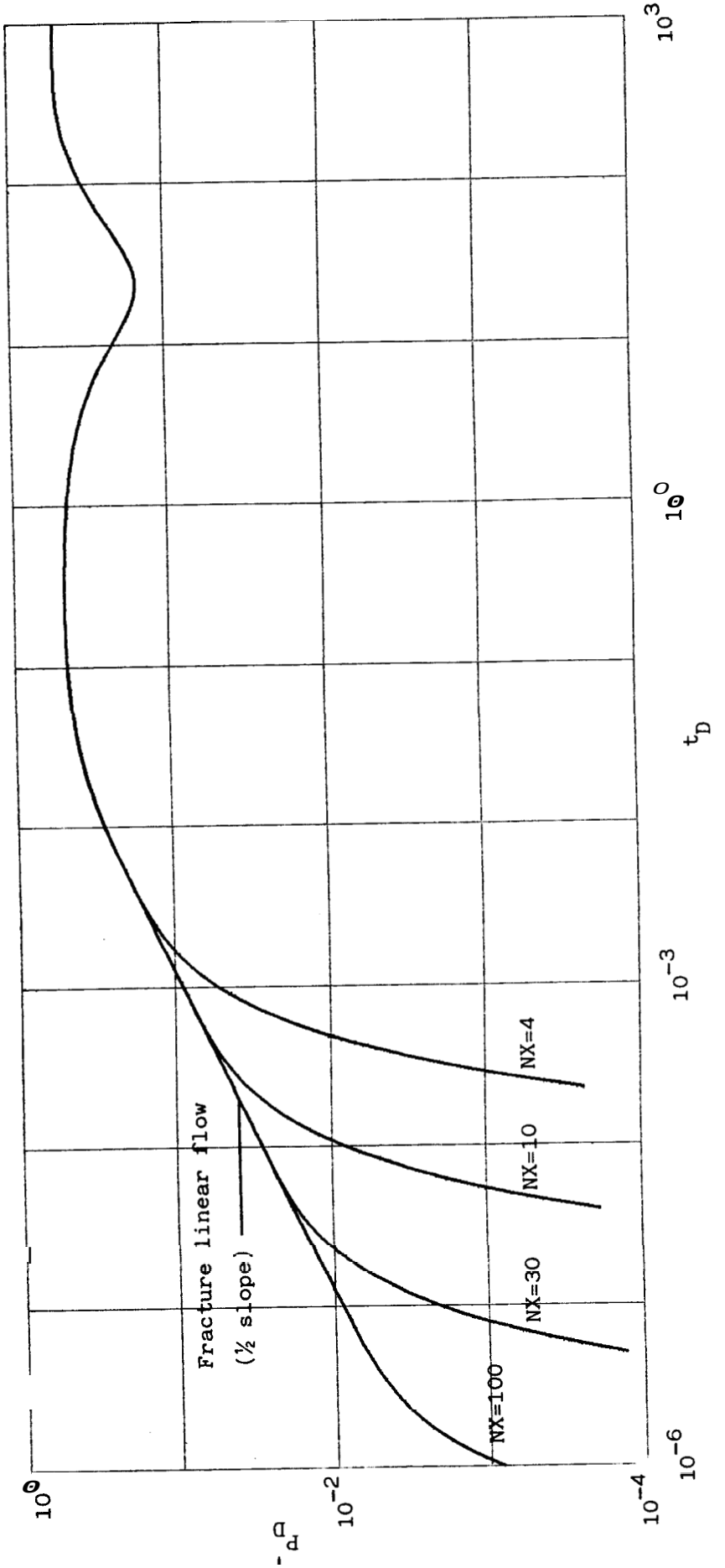

Figure 5–2: Element Green function for different values of X

NE = 1 (Uniform flux)
NX = 100
$\omega = 10^{-2}$
$\lambda = 10^{-4}, 10^{-2}, 100, 102$

$P_D' = t_D . EG$

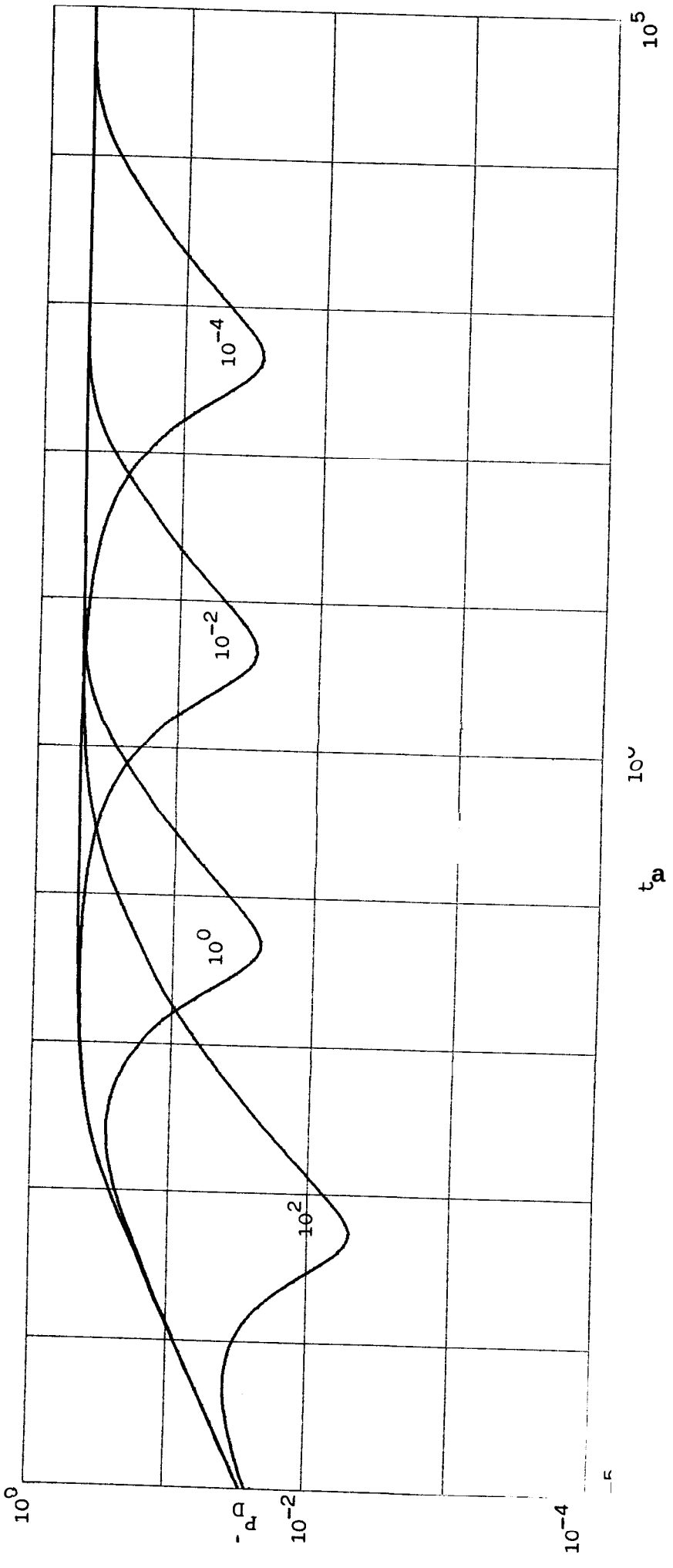

Figure 5–3: Element Green function for different values of ε

NE = 1 (uniform flux)
NX = 100
$a = 10^{-3}$
$\varepsilon = 1, 10^{-1}, 10^{-2}, 10^{-3}$

$P_D' = t_D \cdot EG$

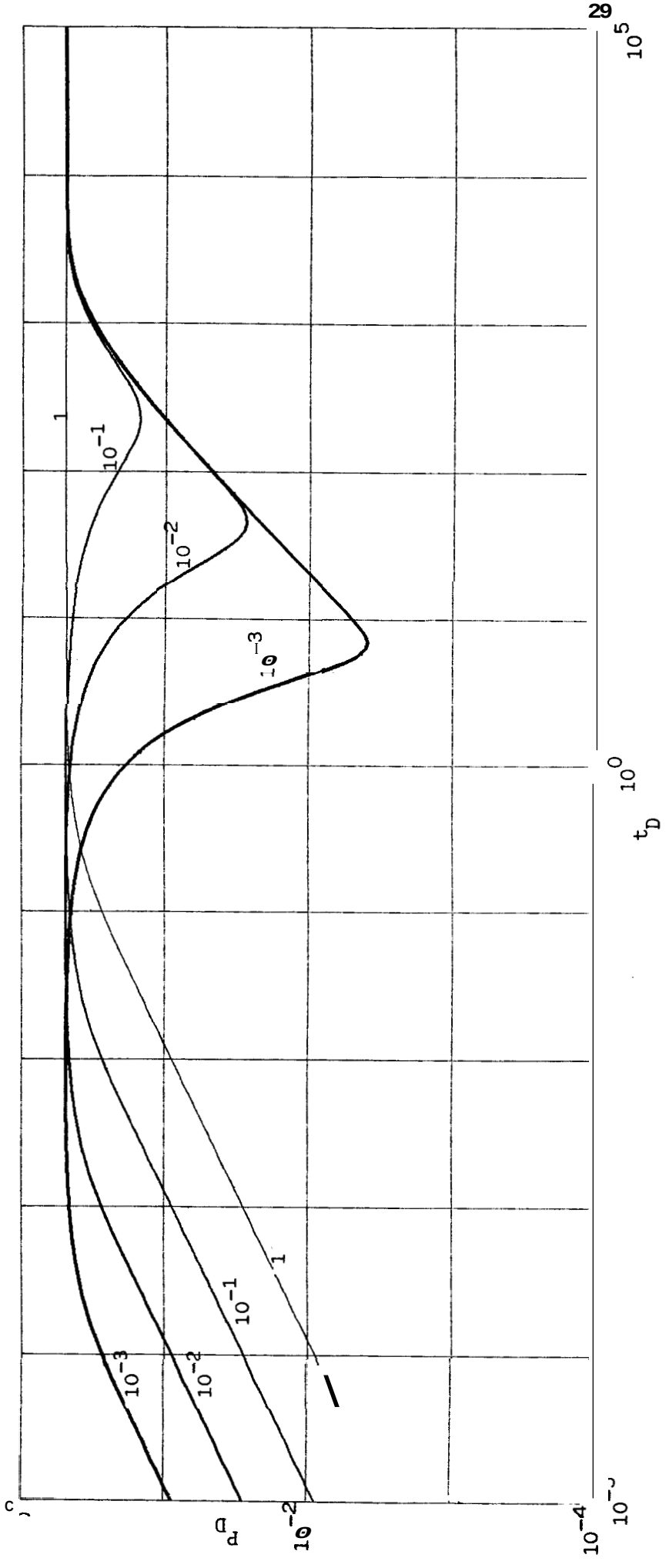

5.3 The Element source solution

We define the function **ES** as the dimensionless element source solution. $ES(x_D,y_D,t_D)$ is the dimensionless pressure drop at the point $M(x_D,y_D)$ at time t_D due to a uniform constant production rate from time Θ to time t_D by an element centered in Θ and of dimensionless length $2/NE$.

ES is the average of the line source solutions on the element. It is given by:

$$ES(x_D,y_D,t_D) = \frac{NE}{2}.\int_{\frac{-1}{NE}}^{\frac{1}{NE}} LS(x_D-u,y_D,t_D).du \qquad (5\text{-}13)$$

The derivation **of** Eq.5-13 with respect to t_D yields:

$$\frac{\partial ES}{\partial t_D}(x_D,y_D,t_D) = \frac{NE}{2}.\int_{\frac{-1}{NE}}^{\frac{1}{NE}} \frac{\partial LS}{\partial t_D}(x_D-u,y_D,t_D).du \qquad (5\text{-}14)$$

Using Eq.4-26 and Eq.5-1, we get:

$$EG(x_D,y_D,t_D) = \frac{\partial ES}{\partial t_D}(x_D,y_D,t_D) \qquad (5\text{-}15)$$

In the same way as EG was computed, the element source solution **is** given by:

$$ES(x_D,y_D,t_D) = \frac{1}{NX}.\sum_{i=1}^{NX} LS(x_D-x_i,y_D,t_D) \qquad (5\text{-}16)$$

The real value ***of*** the pressure drop is given by:

$$p_i - p_f(x,y,t) = \frac{q\mu}{2\pi k_f h}.\ ES(x_D,y_D,t_D) \qquad (5\text{-}17)$$

5.4 The behavior of ES

A typical element source solution is shown in Fig.5-4 for different choices of NX. The late time results are quite accurate, even for low values of NX. The results of early time data produce **a** log-log straight line. The bigger NX **is,** the closer a half slope is approached.

Figure 5–5 shows a typical element source solution for a value of NX large enough to assure numerically correct early time results. NE is taken equal to one (the element has the length of the fracture). The result is compared to the solution for a homogeneous reservoir (ω=1), which is the Gringarten et al. uniform flux type curve. At early times, the flow is linear normal to the fracture. The reservoir reacts as a homogeneous medium of porosity $\omega\Phi$. It follows a homogeneous uniform flux type curve translated in the time. After the transition, the reservoir reacts as a homogeneous medium of porosity Φ. The transition may occur during the linear flow period.

The influence of the storativity ratio ω and the interporosity flow parameter λ are qualitatively the same as for the line source solution. ω determines the fissure flow curve, which is the uniform flux curve for a homogeneous medium translated of $-\log(\omega)$ log-log cycles on the left. λ determines the transition curve from the fissure flow to the total flow.

Figure 5–6 shows several flow and transition curves, and an element source solution for given values of ω and λ.

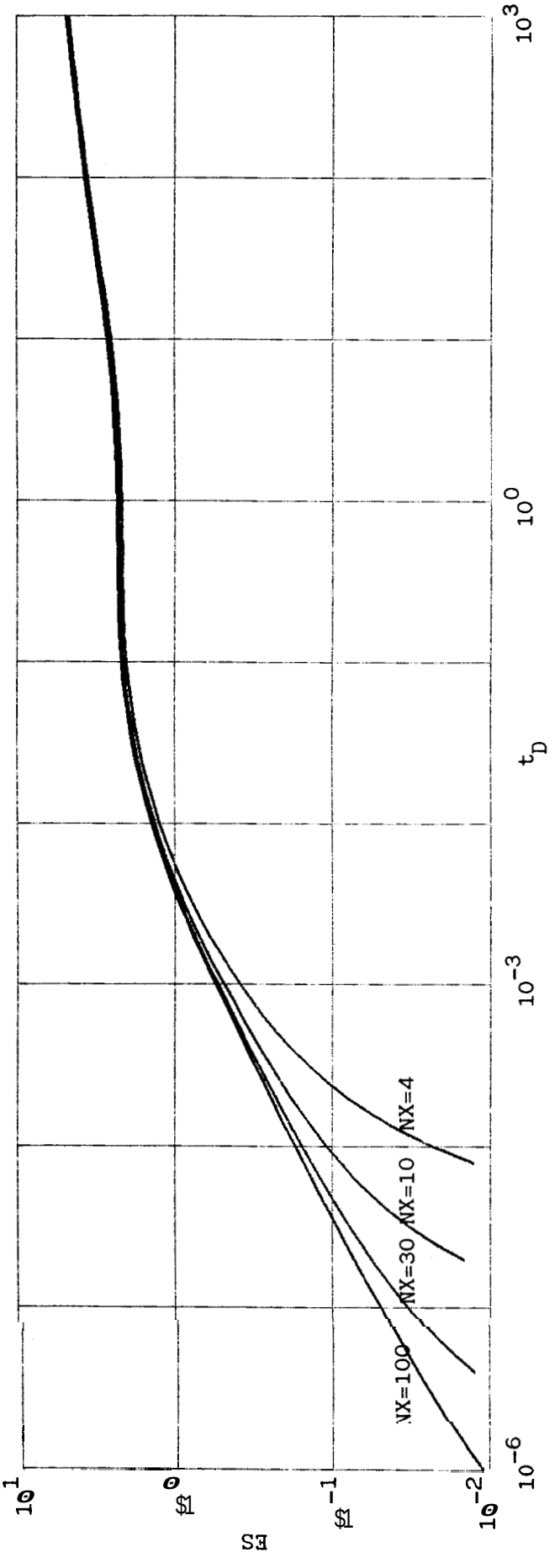

Figure 5-4 : Element source solution for different values of NX.

NE = 1

NX = 4, 10, 30, 100

$\lambda = 10^{-1}$

$\omega = 10^{-2}$

Figure 5-5 : A typical element source solution.

NE = 1

NX = 100

$\lambda = 10^{-2}$

$\omega = 10^{-2}$

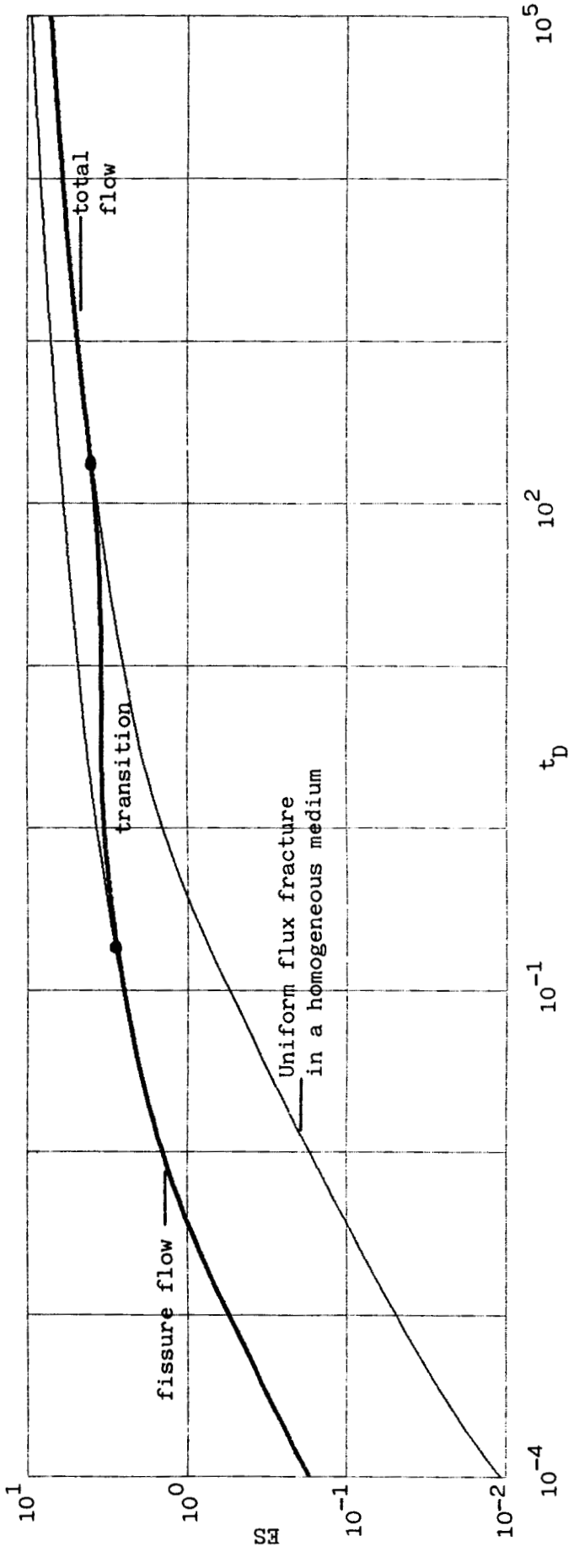

Figure 5-6 : **Flow curves and transition curves for the element source solution.**

NE = 1 (uniform flux fracture)

NX = 100

$\lambda = 10^{-4}, 10^{-2}, 10^{0}, 10^{2}$

$\omega = 10^{-3}, 10^{-2}, 10^{-1}, 1$

Thick curve: $\omega=10^{-2}$, $\lambda=10^{-2}$

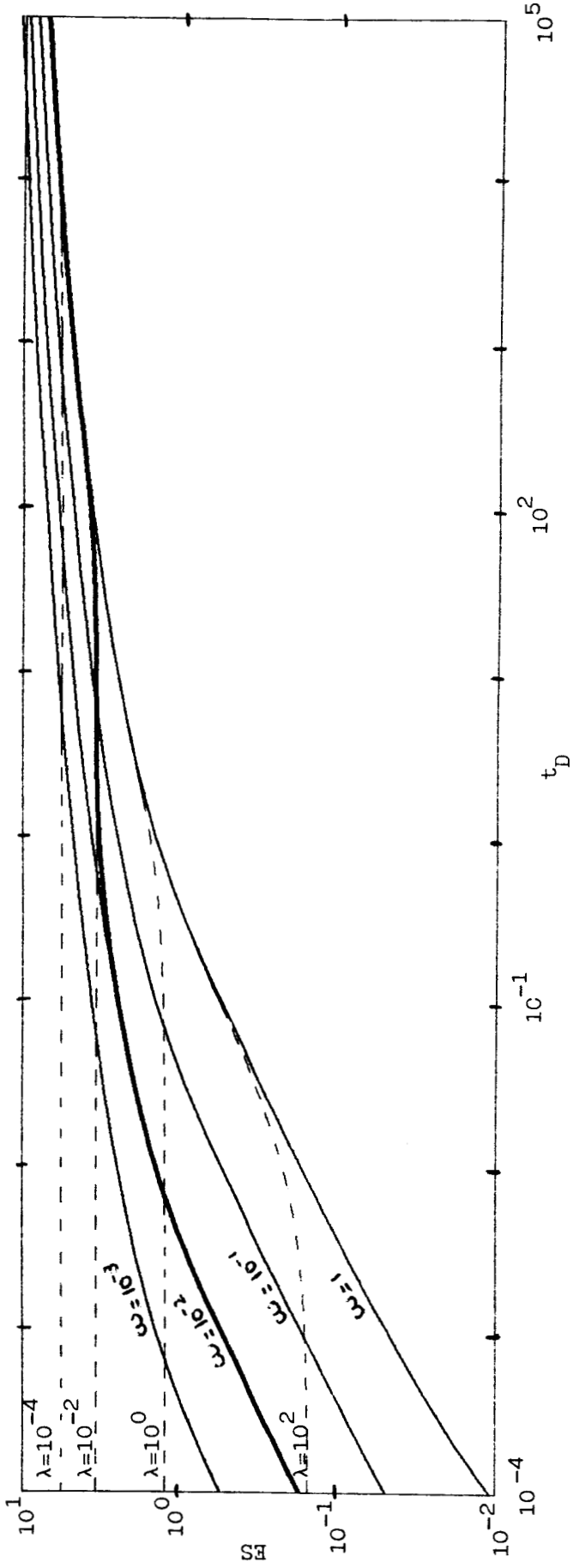

6. INFINITE CONDUCTIVITY FRACTURE IN A DOUBLE-POROSITY MEDIUM

The element source solution and the element Green function were studied in section 5 with NE=1 (the element had the length of the fracture). Therefore, these results are valid for the uniform-flux fracture problem.

$ES_{NE=1}(x_D, y_D, t_D)$ is the dimensionless pressure drop at the point $M(x_D, y_D)$ at time t_D due to the production at constant rate from time 0 to time t_D of a uniform-flux fracture.

$EG_{NE=1}(x_D, y_D, t_D)$ is the dimensionless pressure drop at the point $M(x_D, y_D)$ at time t_D due to a uniform source of total dimensionless strength 1 produced by a uniform-flux fracture at time 0. It is also the dimensionless pressure derivative due to the production at constant rate from time 0 to time t_D.

We are interested in the infinite conductivity case.

6.1 Simulation of the fracture behavior

A simulation of the problem was tried, using the same princip that Gringarten et al. used for the homogeneous case. The fracture was cut in NE elements in which the flux wasassumed to be uniform. From time t_n to time t_{n+1}, the total rate of fluid in the element m was called $q_{n,m}$ and were computed by equating the pressures at time t_{n+1}.

Two problems occured which made this simulation impossible. The first problem was the cost of the program. The influence of the production of $q_{n,m}$ on the element m' is given by the difference of two ES functions, and needs 2.NX Stehfest numerical inversions. We need NE of these operations to compute the influence of the production of the whole fracture from time t_n to time t_{n+1} on the element m' at time t_N, and NE times more to know the influence of the production of the whole fracture from time t_n to time t_{n+1} on all the elements at time t_N. We already reach the number of $2.NX.NE^2$. To know all the influences of the previous productions at time t_N, we need N of the previous calculations. After calculating all the pressures at time t_N, we have to correct all the terms $q_{N-1,m}$ to reach the same pressure everywhere and run an other iteration. In the best cases, we will need 4 iterations to get to a good result. Therefore, we need $8.N.NX.NE^2$ numerical inversions to get from

time t_{N-1} to time t_N, and thus $4.N.(N+1).NX.NE^2$ numerical inversions to get from time zero to time t_N. We need 8 points per log cycle to produce a reliable type curve, and this curve is very long (10 log cycles). Therefore, we reach the number of $4.80.81.NX.NE^2$. Assuming that NX=100 and NE=20, we need 10^9 Stehfest numerical inversions to generate a curve for only given values of ω and χ. The second problem is the reliability of the results. Even for a large NX, the early time results are not accurate, and there is no way to control the effect of this inaccuracy on the results. For all these reasons, the project of a simulation was abandonned.

6.2 Infinite conductivity fracture assumption

Gringarten et al. showed that, for a homogeneous medium, the pressure drop in an infinite conductivity fracture was the same as the pressure drop measured at the point $(0.732\ X_F, 0)$ in the uniform flux fracture. This approximation is still valid during the fissure flow and after the transition in a double porosity medium, as the medium reacts as an homogeneous medium during these periods. The time of the transition is not affected by the model we take: We saw in the figure 4–3 that the time of the transition is not influenced by the distance from the source. Therefore, a difference of repartition of the rates will not change the time of transition. We can expect that Gringarten et al. approximation for a homogeneous medium is still valid for a double–porosity medium.

6.3 Numerical check of the results

Table 6–1 shows the numerical values of $\sqrt{\pi t_D}$, the uniform flux fracture in a homogeneous medium function, the infinite conductivity fracture in a homogeneous medium function (both from Gringarten's program), the uniform flux fracture in a double–porosity medium (ω=1) function and the infinite conductivity fracture in a double–porosity medium (ω=1) function. We see that the results for homogeneous and heterogeneous models fit within 1 percent for t_D greater than 10. The fit gets closer when we increase NX.

6.4 Type-curve with reference to the total system

All the previous study was made taking t_D as defined in Eq.4-3. Thus, the reference porosity is the total porosity. For different values of ω, the fissure flow curves will be different, and the total flow curves will be the same, corresponding to the solution for a homogeneous medium.

Figure 6-2 is the type-curve we get by choosing such a reference. The thick curves are the flow curves. They are Gringarten's type-curve translated in the time (on a log-log plot). They are given by:

$$\text{Flow}(\omega, t_D) = \frac{\sqrt{t_D}}{2\sqrt{\omega}}\left[\text{erf}\left(\frac{0.134}{\sqrt{t_D/\omega}}\right)+\text{erf}\left(\frac{0.866}{\sqrt{t_D/\omega}}\right)\right] - 0.067E_1\left(\frac{0.018}{t_D/\omega}\right)-0.433E_1\left(\frac{0.750}{t_D/\omega}\right) \quad (6\text{-}1)$$

The total flow curve corresponds to $\omega=1$. The thin curves are the transition curves they are computed by taking $\omega=0$ and the true value of χ (λ has no influence on the flow curves). For ten log cycles and eight points per cycle, we need 80.NX numerical inversions to generate one of them.

The main drawback of this type-curve is that it is unhandy. The fracture linear flow starts on the fissure flow curves and sometimes end on the total flow curve. We see that only the total flow curve shows a long half-slope straight line. Therefore, a practical use of these curves is impossible. We need to find a way to have all the fissure flows on the same curve. We do that by taking $\omega\Phi$ as the reference porosity.

6.5 Type-curve with reference to the fissures

If we take $\omega\Phi$ as the reference porosity, Eq.4-3 becomes:

$$t_D = \frac{k_f t}{(V\Phi c_t)_f \mu X_F^2} \qquad t_D = \frac{0.000264\ k_f t}{(V\Phi c_t)_f \mu X_F^2} \quad (6\text{-}2)$$

This change yields new dimensionless diffusivity equations which replace Eq.4-9 and Eq.4-10 :

$$\nabla^2 p_{fD} = \frac{\partial p_{fD}}{\partial t_D} + \frac{(1-\omega)}{\omega}\frac{\partial p_{mD}}{\partial t_D} \quad (6\text{-}3)$$

$$\lambda(p_{mD}-p_{fD}) = -\frac{(1-\omega)}{\omega}\frac{\partial p_{mD}}{\partial t_D} \quad (6\text{-}4)$$

After Laplace transformation, **Eq.4-14** and **Eq.4-15** become:

$$\nabla^2 \bar{p}_{fD} = s\bar{p}_{fD} + \frac{1-\omega}{\omega} s\bar{p}_{mD} \qquad (6\text{-}5)$$

$$\bar{p}_{mD} = \frac{\lambda}{\lambda + \frac{1-\omega}{\omega} s}\, \bar{p}_{fD} \qquad (6\text{-}6)$$

Finally, we get **Eq.4-16,** but f(s) is now defined by:

$$f(s) = \frac{\lambda + (1-\omega)s}{\lambda\omega + (1-\omega)s} \qquad (6\text{-}7)$$

All the previous study can be repeated with this new value of f(s). The only difference is that, for different values of ω, all the fissure flow curves will be the same and all the matrix +fissure flow curves will be different. The curve corresponding to a homogeneous medium will be the fissure flow curve, and all the other flow curves will be on the right of the homogeneous curve, instead of being on the left.

Figure **6-3** shows the corresponding type-curve for an infinite conductivity fracture. The thick curves are the flow curves. The top one is the fissure flow curve (Gringarten's homogeneous type curve). The others are the total flow curves, depend on ω and are given by :

$$\text{Flow}(\omega, t_D) = \frac{\sqrt{\pi\omega t_D}}{2}\cdot\left[\text{erf}\left(\frac{0.134}{\sqrt{\omega t_D}}\right)+\text{erf}\left(\frac{0.866}{\sqrt{\omega t_D}}\right)\right] - 0.067E_i\left(\frac{0.018}{\omega t_D}\right)-0.433E_i\left(\frac{0.75}{\omega t_D}\right) \qquad (6\text{-}8)$$

The thin curves are the transition curves and are computed from the double-porosity program. Each of these curves needs 80.NX numerical inversions. The transition curves only depend on the value of λ.

These curves are very long (ten log cycles) . The half slope "uses" a lot of place and we can not assume which part of the curves are practically usefull.

Figure **6-4** shows the same type-curve cut in two parts. Two of these taped together yield Figure **6-3.**

Table **6-1** : Numerical check of the results

column 1 : t_D

column 2 : $\sqrt{\pi t_D}$

column 3 : Uniform flux fracture in a homogeneous medium, from Gringarten et al.

column 4 : Infinite conductivity fracture in a homogeneous medium, from Gringarten et al.

column 5 : Uniform flux fracture in a double-porosity medium, with ω=1.

column 6 : Infinite conductivity fracture in a double-porosity medium, with ω=1.

Td	sqrt(PI*Td)	hom-Qunif	hom-InfCon	hot-Qunif	hot-InfCon
200-01	.2506620D+00	[illegible]	.2455715D+00	[illegible]	[illegible]
400-01	[illegible]	[illegible]	[illegible]	[illegible]	[illegible]
[illegible]	[illegible]	[illegible]	[illegible]	[illegible]	[illegible]
[illegible]	[illegible]	[illegible]	[illegible]	[illegible]	[illegible]
[illegible]	[illegible]	[illegible]	[illegible]	[illegible]	[illegible]
[illegible]	[illegible]	[illegible]	[illegible]	[illegible]	[illegible]
[illegible]	[illegible]	[illegible]	[illegible]	[illegible]	[illegible]
[illegible]	[illegible]	[illegible]	[illegible]	[illegible]	[illegible]
[illegible]	[illegible]	[illegible]	[illegible]	[illegible]	[illegible]
[illegible]	.1772454D+01	[illegible]	[illegible]	[illegible]	[illegible]
[illegible]	.2506620D+01	[illegible]	.1503336D+01	.1764646D+01	[illegible]
[illegible]	[illegible]	[illegible]	.1824382D+01	[illegible]	[illegible]
[illegible]	[illegible]	[illegible]	[illegible]	.2300405D+01	.2011983D+01
[illegible]	.5013257D+01	[illegible]	.2158427D+01	[illegible]	[illegible]
100+02	[illegible]	[illegible]	.2207349D+01	.2553069D+01	[illegible]
200+02	[illegible]	.2904405D+01	.2608581D+01	[illegible]	.2601596D+01
400+02	[illegible]	.3250021D+01	.2952461D+01	.3243105D+01	[illegible]
600+02	.1372337D+02	.3452407D+01	.3154293D+01	.3445491D+01	[illegible]
800+02	.1585331D+02	.3596075D+01	.3297683D+01	[illegible]	[illegible]
100+03	.1772454D+02	.3707543D+01	.3408984D+01	[illegible]	[illegible]
200+03	.2506620D+02	.4053910D+01	.3755017D+01	[illegible]	.3748030D+01
400+03	[illegible]	[illegible]	.4101320D+01	[illegible]	.4094332D+01
600+03	.4341608D+02	.4693074D+01	.4303962D+01	[illegible]	[illegible]
800+03	.5013257D+02	.4746902D+01	.4447759D+01	[illegible]	[illegible]
100+04	.5604991D+02	.4858464D+01	.4559303D+01	[illegible]	[illegible]

Figure 6–2 : Infinite conductivity fracture in a double–porosity medium – reference to the total system.

$$t_D = \frac{k_f t}{[(V\Phi c_t)_f + (V\Phi c_t)_m]\mu X_F^2}$$

$$p_D = \frac{2\pi k_f h}{q\mu}(p_i - p)$$

Flow curves (thick): $10^{-3} \leqslant \omega \leqslant 100$

Transition curves (thin):

NX = 100

$10^{-5} \leqslant \lambda \leqslant 10^{3}$

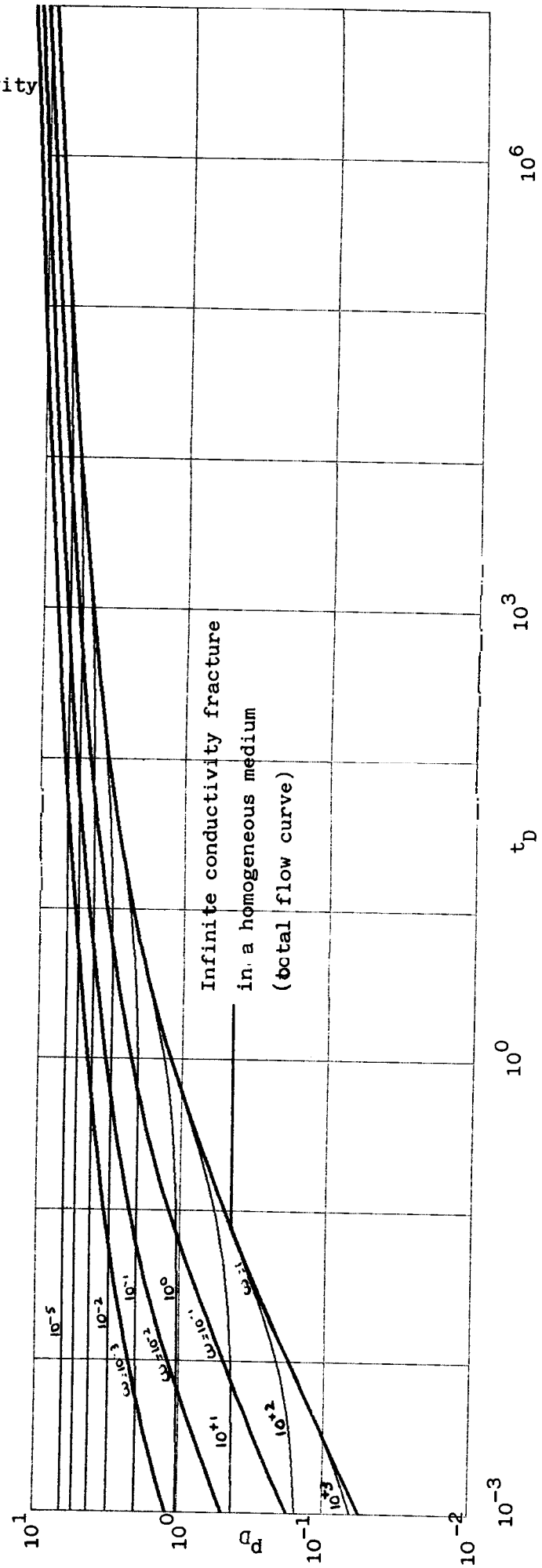

Figure 6–3 : Infinite conductivity fracture in a double–porosity medium – reference to the fissured system.

$$t_D = \frac{k_f t}{(V\Phi c_t)_f \mu X_F^2}$$

$$p_D = \frac{2\pi k_f h}{q\mu}(p_i - p)$$

Flow curves (thick): $10^{-3} \leqslant \omega \leqslant 10^{0}$

Transition curves (thin):

NX = 100

$10^{-5} \leqslant \lambda \leqslant 103$

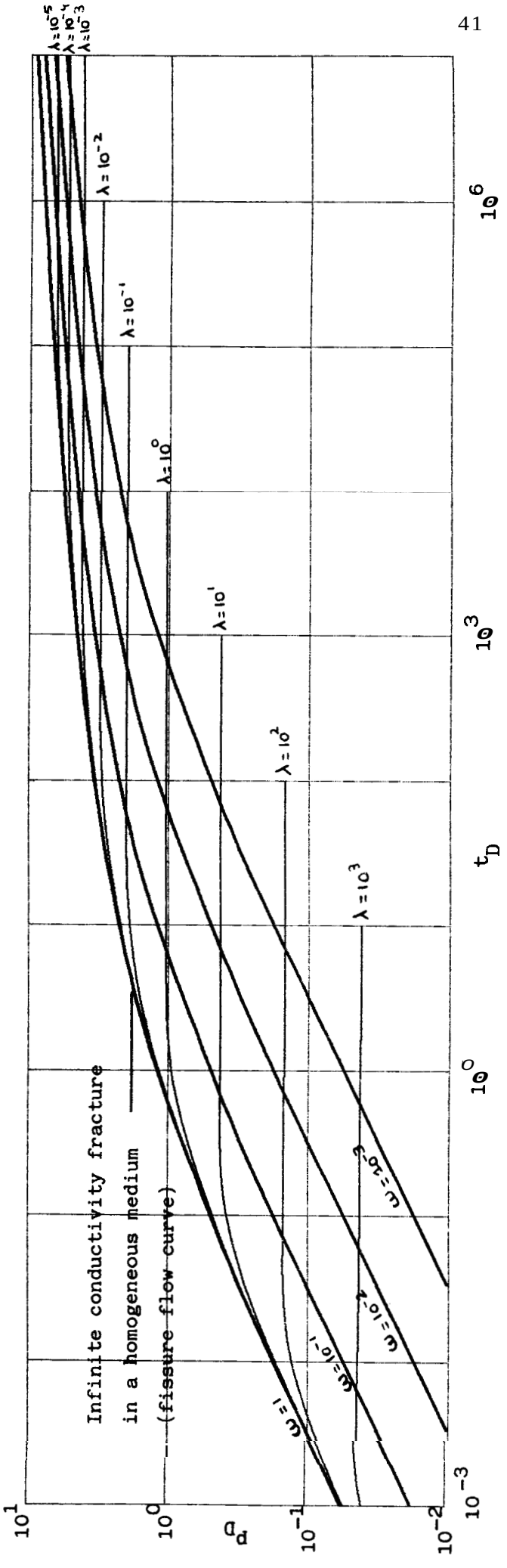

Figure 6-4: Infinite conductivity fracture in a double-porosity medium

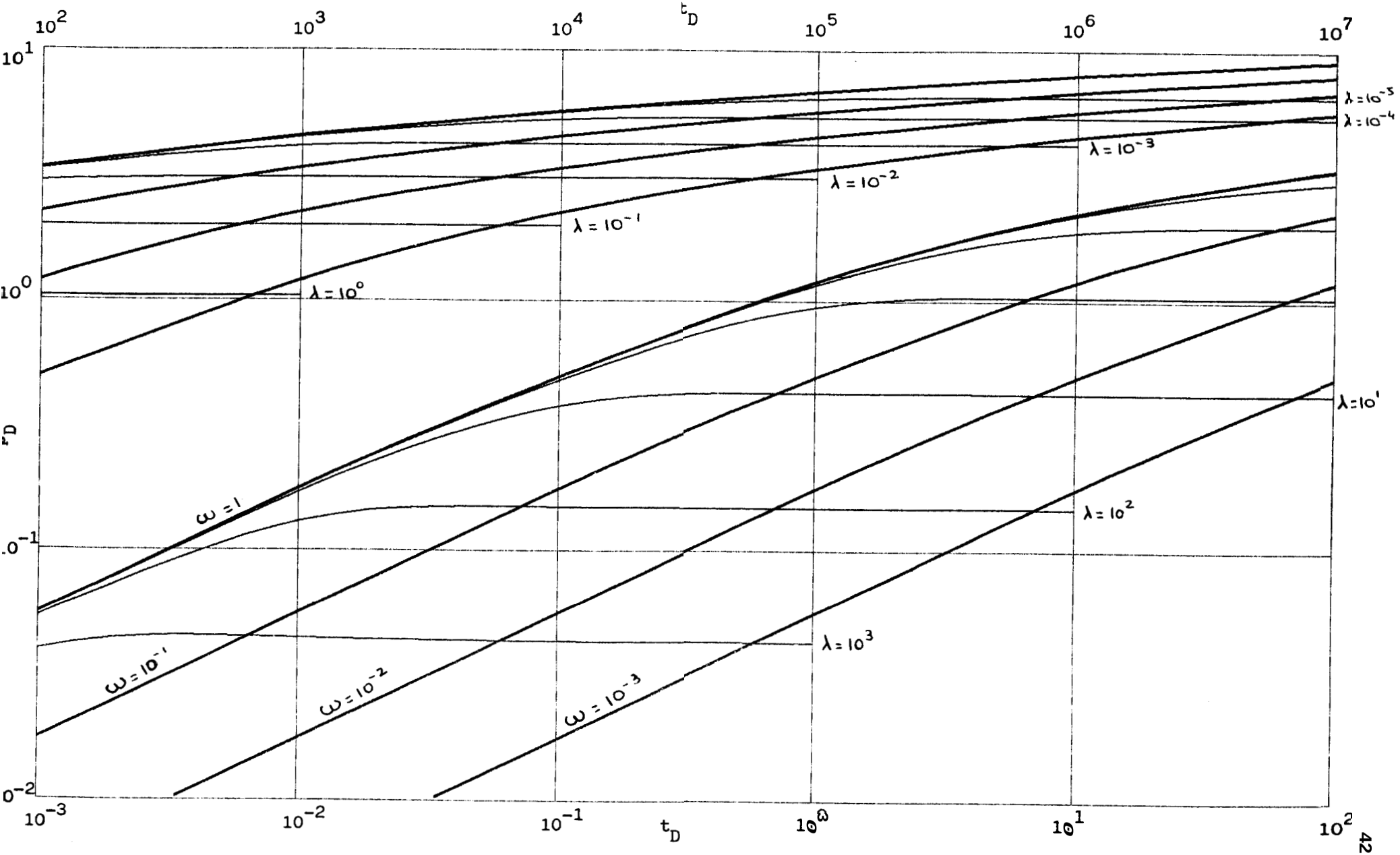

7. NOMENCLATURE

7.1 Subscripts

f : Related to the fissures

F : Related to the fracture

m : Related to the matrix medium

D : dimensionless

7.2 Latin

B	: Reservoir volume factor	dimensionless
c	: fluid isothermal compressibility	$M^{-1}.L.T^2$
c_f	: formation isothermal compressibility	$M^{-1}.L.T^2$
c_t	: total isothermal compressibility	$M^{-1}.L.T^2$
EG	: Element Green function	dimensionless
ES	: Element source solution	dimensionless
f	: Function in Laplace space	dimensionless
h	: Formation thickness	L
I_0	: Modified Bessel function	
k	: Permeability	L^2
K_0	: Modified Bessel function	
LG	: Line Green function	dimensionless
LS	: Line source solution	dimensionless
NE	: Number of elements in the fracture	
NX	: Number of points in an element	
O	: Center of the fracture	
p	: Pressure	$ML^{-1}T^{-2}$
p_i	: Initial pressure in the reservoir	$ML^{-1}T^{-2}$
p_s	: Reference pressure	$ML^{-1}T^{-2}$
q_*	: Volumetric flowrate	L^3T^{-1}
q	: Volumetric flow rate from the matrix to the fissures per unit of bulk volume	T^{-1}
r	: Distance from O	L
s	: Laplace variable	dimensionless
t	: time	T
u	: Darcy velocity	LT^{-1}
V	: ratio of a medium volume to the total bulk volume	dimensionless
X_F	: Fracture half length	L
x,y	: Cartesian coordinates from the point O	L

7.3 Greek

a	Interporosity flow shape factor	L^{-2}
λ	Interporosity flow parameter	dimensionless
ω	Ratio of storativities	dimensionless
μ	Fluid viscosity	$ML^{-1}T^{-1}$
Φ	Total porosity	dimensionless
ρ	Fluid density	ML^{-3}

8. REFERENCES

Abramowitz, M., and Stegun, I.A. : Handbook of mathematical functions, Dover Publications, inc., New York, 9th Edition (1970).

Carslaw, A.C., and Jaeger, J.C. : Conduction of heat in solids, New York, Oxford University Press, 2nd edition (1959).

Deruyck, B.G., Bourdet, D.P., DaPrat, G., and Ramey, H.J.Jr : "Interpretation of Interference Tests in Reservoirs with Double-Porosity Behavior - Theory and Field Examples", Paper SPE N°11025, Proceedings, 57th Annual Fall Meeting, SPE of AIME, New Orleans, LA, Sept. 26-29, 1982.

Gringarten, A.C., Ramey, H.J.Jr : "Unsteady-state Pressure Distributions created by a well with a single infinite-conductivity vertical Fracture", SPE Jour. (August, 1974).

Stehfest, H. : "Algorithm 368: Numerical inversion of Laplace Transform", Communication of the A.C.M. (1970), 1, N°13.

Warren, J.E., and Root, P.J.: "The Behavior of Naturally Fractured Reservoirs", SPE Jour. (September 1963), 245-255.

9. APPENDIX A: FORTRAN PROGRAMS

9.1 Line source solution program

Subroutines needed : Modified Bessel function K_0 (p.52)

```
C*************************************************************************
C                    LINE SOURCE SOLUTION
C*************************************************************************
C
C     This function gives the variation of pressure at the point
C     M (located at the distance Rd*L from O) at time Td due to
C     a constant rate produced at the point O from time Ø to time
C     Td in a double porosity medium.
C
C
C                                  + M (Xd,Yd)
C                                 /
C                                /
C                               / Rd
C                              /
C                             /
C                            +
C                            O (Ø,Ø)
C
C     The input parameters are
C
C           * RD     : dimensionless distance from O to M
C           * TD     : dimensionless time
C           * N,M    : control parameters for the Stehfest
C                      algorithm
C           * W      : ratio of the storativities
C           * LAMBDA: interporosity flow parameter
C*************************************************************************
C
      DOUBLE PRECISION FUNCTION SRCE(RD,TD,N,M,W,LAMBDA)
      IMPLICIT REAL*8 (A-H,O-Z)
      REAL*8 LAMBDA
      DIMENSION G(5Ø),V(5Ø),H(25)
C
C     Test of first call
      IF (N.EQ.M) GOTO 213
C
C     Initialisation of the arrays
      M=N
      DLOGTW=.693147180Ø5599
      NH=N/2
      G(1)=1.
      DO 2Ø1 I=2,N
      G(I)=G(I-1)*I
2Ø1   H(1)=2./G(NH-1)
      DO 2Ø4 I=2,NH
      FI=I
      IF (I-NH) 2Ø2,2Ø3,2Ø4
2Ø2   H(I)=FI**NH*G(2*I)/(G(NH-I)*G(I)*G(I-1))
      GOTO 2Ø4
2Ø3   H(I)=FI**NH*G(2*I)/(G(I)*G(I-1))
2Ø4   CONTINUE
      SN=2*(NH-NH/2*2)-1
      DO 212 I=1,N
      V(I)=Ø.
      K1=(I+1)/2
      K2=I
```

```
      IF (K2-NH) 206,206,205
205   K2=NH
206   DO 211 K=K1,K2
      IF (2*K-I) 207,209,207
207   IF (I-K) 208,210,208
208   V(I)=V(I)+H(K)/(G(I-K)*G(2*K-I))
      GOTO 211
209   V(I)=V(I)+H(K)/G(I-K)
      GOTO 211
210   V(I)=V(I)+H(K)/G(2*K-I)
211   CONTINUE
      V(I)=SN*V(I)
      SN=-SN
212   CONTINUE
C
C     Computing the Laplace transform of PF
213   SRCE=0.
      A=DLOGTW/TD
      DO 214 I=1,N
      ARG=A*I
      SRCE=SRCE+V(I)*PFD(RD,ARG,W,LAMBDA)
214   CONTINUE
      SRCE=SRCE*A
      RETURN
      END
C
C*****************************************************************
C
C
      DOUBLE PRECISION FUNCTION PFD(R,S,W,LAMBDA)
      IMPLICIT REAL*8 (A-H,O-Z)
      REAL*8 LAMBDA
      U=FWL(S,W,LAMBDA)
      X=R*DSQRT(S)*DSQRT(U)
      PFD=SK0(X)/S
      RETURN
      END
C
C*mm*** *******************************************************
C
C
      DOUBLE PRECISION FUNCTION FWL(S,W,LAMBDA)
      IMPLICIT REAL*8 (A-H,O-Z)
      REAL*8 LAMBDA
      FWL=(W*(1-W)*S+LAMBDA)/((1-W)*S+LAMBDA)
      RETURN
      END
C
C*****************************************************************
```

9.2 Line Green function program

Subroutines needed : Modified Bessel function K_0 (p.52)

```
C*************************************************************************
C                    LINE GREEN FUNCTION
C*************************************************************************
C
C
C       This function gives the variation of pressure at the point
C       M (located at the distance Rd*L from O) at time Td due to
C       an impulsion of unit strength at the point O at time 0 in a
C       double porosity medium.
C
C
C                                  + M (Xd Yd)
C                                 /
C                                /
C                               / Rd
C                              /
C                             /
C                            +
C                            O (0,0)
C
C
C       The input parameters are:
C
C            * RD     : dimensionless distance from O to M
C            * TD     : dimensionless time
C            * N,M    : control parameters for the Stehfest
C                       algorithm
C            * W      : ratio of the storativities
C            * LAMBDA: interporosity flow parameter
C
C*************************************************************************
C
      DOUBLE PRECISION FUNCTION GREEN(RD,TD,N,M,W,LAMBDA)
      IMPLICIT REAL*8 (A-H,O-Z)
      REAL*3 LAMBDA
      DIMENSION G(50),V(50),H(25)
C
C     Test of first call
      IF (N.EQ.M) GOTO 213
C
C     Initialisation of the arrays
      M=N
      DLOGTW=.693147180559
      NH=N/2
      G(1)=1.
      DO 201 I=2,N
201   G(I)=G(I-1)*I
      H(1)=2./G(NH-1)
      DO 204 I=2,NH
      F1=1
      IF (I-NH) 202,202,203,204
202   H(I)=F1**NH*G(2*I)/(G(NH-I)*G(I)*G(I-1))
      GOTO 204
203   H(I)=F1**NH*G(2*I)/(G(I)*G(I-1))
204   CONTINUE
      SN=2*(NH-NH/2*2)-1
      DO 212 I=1,N
      V(I)=0.
      K1=(I+1)/2
      K2=I
```

```
      IF (K2-NH) 206,206,205
205   K2=NH
206   DO 211 K=K1,K2
      IF (2*K-I) 207,209,207
207   IF (I-K) 208,210,208
208   V(I)=V(I)+H(K)/(G(I-K)*G(2*K-I))
      GOTO 211
209   V(I)=V(I)+H(K)/G(I-K)
      GOTO 211
210   V(I)=V(I)+H(K)/G(2*K-I)
211   CONTINUE
      V(I)=SN*V(I)
      SN=-SN
212   CONTINUE
C
C     Computing the Laplace transform of PFD
213   GREEN=0.
      A=DLOGTW/TD
      DO 214 I=1,N
      ARG=A*I
      GREEN=GREEN+V(I)*PFD(RD,ARG,W,LAMBDA)
214   CONTINUE
      GREEN=GREEN*A
      RETURN
      END
C
C*************************************************************************
C
C
      DOUBLE PRECISION FUNCTION PFD(R,S,W,LAMBDA)
      IMPLICIT REAL*8 (A-H,O-Z)
      REAL*8 LAMBDA
      U=FWL(S,W,LAMBDA)
      X=R*DSQRT(S)*DSQRT(U)
      PFD=SK0(X)
      RETURN
      END
C
C*************************************************************************
C
C
      DOUBLE PRECISION FUNCTION FWL(S,W,LAMBDA)
      IMPLICIT REAL*8 (A-H,O-Z)
      REAL*8 LAMBDA
      FWL=(W*(1-W)*S+LAMBDA)/((1-W)*S+LAMBDA)
      RETURN
      END
C
C*************************************************************************
```

9.3 Element source solution program

Subroutines needed : Line source solution program (p.46)
Modified Bessel function K_0 (p.52)

```
C**********************************************************************
C                     ELEMENT SOURCE SOLUTION
C**********************************************************************
C
C
      DOUBLE PRECISION FUNCTION ESRCE(XD,YD,TD,NE,NX,N,M,W,LAMBDA)
C
C
C**********************************************************************
C
C     This function gives the variation of pressure at the point
C     M (Xd,Yd) at time Td due to a constant and uniform flow
C     rate produced by an element of fracture, of length 2/Ne,
C     centered in O, in the X direction, produced from time Ø to
C     time Td, in a double porosity medium.
C
C
C                                     + M (Xd,Yd)
C
C
C
C                -1                 0                1
C       ---------|----------------===+===------------|---------->x
C                                <----->
C                                   !____ Element
C              <------------------------------------>
C                                   !_____Fracture
C
C
C     The input parameters are:
C
C           * XD,YD  : dimensionless coordinates of M
C           * TD     : dimensionless time
C           * NE     : number of elements in a fracture
C           * NX     : number of parts we cut the element
C           * N,M    : control parameters for the Stehfest
C                      algorithm
C           * W      : ratio of the storativities
C           * LAMBDA:  interporosity flow parameter
C
C**********************************************************************
C
C
      IMPLICIT REAL*8 (A-H,O-Z)
      REAL*8 LAMBDA
      DIMENSION XX(1ØØ)
      DX=2./(NE*NX)
      DO 51 I=1,NX
51    XX(I)=-1./NE-DX/2+I*DX
      ESRCE=Ø.
      DO 52 I=1,NX
      RD=DSQRT((XX(I)-XD)**2+YD**2)
52    ESRCE=ESRCE+SRCE(RD,TD,N,M,W,LAMBDA)/NX
      RETURN
      END
C
C
C**********************************************************************
```

9.4 Element Green function program

Subroutines needed : Line Green function program (p.48)

Modified Bessel function K_0 (p.52)

```
C***********************************************************************
C                          ELEMENT GREEN FUNCTION
C***********************************************************************
C
C
      DOUBLE PRECISION FUNCTION EGREEN(XD,YD,TD,NE,NX,N,M,W,LAMBDA)
C
C
C***********************************************************************
C
C     This function gives the variation of pressure at the point
C     M (Xd,Yd) at time Td due to a unit strength impulsion produced
C     at time Ø by an element of fracture, of length 2/Ne, centered
C     in O, in the X direction, in a double porosity medium.
C
C
C                                            + M (Xd,Yd)
C
C
C
C                   -1                  O               1
C          ---------|----- -----===+===----------|------------>x
C                                  <----->
C                                     !____ Element
C                        <-------------------------------->
C                                     !_____Fracture
C
C
C     The input parameters are:
C
C               * XD,YD : dimensionless coordinates of M
C               * TD    : dimensionless time
C               * NE    : number of elements in a fracture
C               * NX    : number of parts we cut the element
C               * N,M   : control parameters for the Stehfest
C                         algorithm
C               * W     : ratio of the storativities
C               * LAMBDA: interporosity flow parameter
C
C***********************************************************************
C
C
      IMPLICIT REAL*8 (A-H,O-Z)
      REAL*8 LAMBDA
      DIMENSION XX(1ØØ)
      DX=2./(NE*NX)
      DO 51 I=1,NX
51    XX(I)=-1./NE-DX/2+I*DX
      EGREEN=Ø.
      DO 52 I=1,NX
      RD=DSQRT((XX(I)-XD)**2+YD**2)
52    EGREEN=EGREEN+GREEN(RD,TD,N,M,W,LAMBDA)/NX
      RETURN
      END
C
C
C***********************************************************************
```

9.5 Modified Bessel function K_0

Subroutines needed : none

```
C*****************************************************************
C
C
      DOUBLE PRECISION FUNCTION SKØ(ARG)
      IMPLICIT REAL*8 (A-H,O-Z)
      DIMENSION F(4),G(3),P(6),PP(1Ø),Q(2),QQ(1Ø)
      DATA CONST/.11593151565841244 9D+ØØ/
      DATA XINF/1.7D+38/
      DATA XMAX/87.4ØDØ/
      DATA XSMALL/2.117582368D-22/
      DATA P/.5859922141282612ØØØD-Ø3, .1316605256498957 18D+ØØ,
     *       .1199946372491Ø7141D+Ø2, .4685Ø9Ø12Ø19348321D+Ø3,
     *       .591690598522705122D+Ø4, .2470815272Ø3995526D+Ø4/
      DATA Q/-.2499441897283230 36D+Ø3, .2131271430384912Ø3D+Ø5/
      DATA F/-.1641445283729 9Ø641D+Ø1,-.296Ø16578929588438D+Ø3,
     *       -.177337846849529859D+Ø5,-.4Ø32Ø34Ø761145482 2D+Ø6/
      DATA G/-.25Ø6497244587799 27D+Ø3, .2986571316305 4Ø254D+Ø5,
     *       -.1612813630445819 4ØD+Ø7/
      DATA PP/.1139498Ø557384 7782D+Ø3, .36832589957340 2679D+Ø4,
     *        .31Ø754Ø898Ø6843923D+Ø5, .1Ø577Ø68948Ø34Ø219D+Ø5,
     *        .1739886790 25656862D+Ø6, .15Ø97646353289 1450D+Ø5,
     *        .71557Ø62783764Ø375D+Ø5, .183215258701835377D+Ø5,
     *        .23444738764199315ØD+Ø4, .116ØØ249425Ø76Ø355D+Ø3/
      DATA QQ/.2ØØ13443Ø649492424D+Ø3, .44329628889746 4Ø87D+Ø4,
     *        .31474655750295 2788D+Ø5, .97418829762268Ø7580D+Ø5,
     *        .15144644673520 1578D+Ø6, .1268983958797 75987D+Ø6,
     *        .588246167858 57Ø276D+Ø5, .1484722837180236Ø9D+Ø5,
     *        .18821890840982 7137D+Ø4, .925565991773Ø48397D+Ø2/
      X=ARG
      IF (X.GT.XMAX) GOTO 45
      IF (X.GT.1.ØDØ) GOTO 25
      TEMP=DLOG(X)
      IF (X.LT.XSMALL) GOTO 2Ø
      XX=X*X
      SUMP=((((P(1)*XX+P(2))*XX+P(3))*XX+P(4))*XX+P(5))*XX+P(6)
      SUMQ=(XX+Q(1))*XX+Q(2)
      SUMF=((F(1)*XX+F(2))*XX+F(3))*XX+F(4)
      SUMG=((XX+G(1))*XX+G(2))*XX+G(3)
      SKØ=SUMP/SUMQ-XX*SUMF*TEMP/SUMG-TEMP
      RETURN
   2Ø SKØ=CONST-TEMP
      RETURN
   25 XX=1.ØDØ/X
      SUMP=PP(1)
      DO 3Ø I=2,1Ø
      SUMP=SUMP*XX+PP(I)
   3Ø CONTINUE
      SUMQ=XX
      DO 35 I=1,9
      SUMQ=(SUMQ+QQ(I))*XX
   35 CONTINUE
      SUMQ=SUMQ+QQ(1Ø)
      SKØ=SUMP/SUMQ/DSQRT(X)
      SKØ=SKØ*DEXP(-X)
      RETURN
   45 SKØ=Ø.ØDØ
      RETURN
      END
C*****************************************************************
```

9.6 Fracture behavior in a double-porosity medium

Subroutines needed : Element source solution program (p.50)

Line source solution program (p.46)

Modified Bessel function K_0 (p.52)

```
C*****************************************************************
C           FRACTURE BEHAVIOR IN A DOUBLE POROSITY MEDIUM
C*****************************************************************
C
C      From: " INFINITE CONDUCTIVITY FRACTURE IN A NATURALLY
C      FRACTURED RESERVOIR " --- HOUZE , HORNE , RAMEY : April 1984
C
       DOUBLE PRECISION FUNCTION FRACHET(IOPT,TD,NX,N,M,W,LAMBDA)
C
C      This function gives the variation of pressure at the point O
C      at time Td due to a constant flow rate produced by fracture,
C      of length 2.Xf (dimensionless length 2. , centered in O, in
C      the X direction, produced from time Ø to time Td, in a double
C      porosity medium. The fracture may be uniform flux (IOPT=Ø) or
C      of infinite conductivity (IOPT=1).
C
C                   -1                 0                  1
C        ----------|==================+==================|----------->x
C                  <------------------------------------->
C                                     :_____Fracture
C      The input parameters are:
C             * IOPT  : nature of fracture parameter
C             * TD    : dimensionless time
C             * NX    : number of parts we cut the fracture
C             * N,M   : control parameters for the Stehfest algorithm
C             * W     : ratio of the storativities
C             * LAMBDA: interporosity flow parameter
C
       IMPLICIT REAL*8 (A-H,O-Z)
       REAL*8 LAMBDA
       DIMENSION XX(1ØØ)
       XD=Ø.
       IF(IOPT.EQ.1) XD=.732
       IF(IOPT.EQ.1) GOTO 2
       DX=2./NX
       DO 1 I=1,NX
1      XX(I)=-1.-DX/2+I*DX
       GOTO 5
2      A=NX*1.732/2
       B=2*(A-DFLOAT(INT(A)))
       N1=INT(A)+INT(B)
       N2=NX-N1
       DX1=1.732/N1
       DX2=.268/N2
       DO 3 I=1,N1
3      XX(I)=-1.-DX1/2+I*DX1
       DO 4 I=1,N2
4      XX(N1+I)=.732-DX2/2+I*DX2
5      FRACHET=Ø.
       IF(IOPT.EQ.1) GOTO 7
       DO 6 I=1,NX
       RD=DSQRT((XX(I)-XD)**2+YD**2)
6      FRACHET=FRACHET+SCE(RD,TD,N,M,W,LAMBDA)/NX
       RETURN
       RD=DSQRT((XX(I)-XD)**2+YD**2)
8      FRACHET=FRACHET+SCE(RD,TD,N,M,W,LAMBDA)*1.732/(2*N1)
       DO 9 I=1,N2
       RD=DSQRT((XX(N1+I)-XD)**2+YD**2)
9      FRACHET=FRACHET+SCE(RD,TD,N,M,W,LAMBDA)*.268/(2*N2)
       RETURN
       END
```